

Supplementary Information

Bioorthogonal Dissociative Rhenium(I) Photosensitisers for Controlled Immunogenic Cell Death Induction

Guang-Xi Xu,^a Lawrence Cho-Cheung Lee,^{a,b} Peter Kam-Keung Leung,^{a,c} Eunice Chiu-Lam Mak,^a Justin Shum,^a Kenneth Yin Zhang,^d Qiang Zhao^d and Kenneth Kam-Wing Lo^{*a,c}

^a Department of Chemistry, City University of Hong Kong, Tat Chee Avenue, Kowloon, Hong Kong, P. R. China; E-mail: bhkenlo@cityu.edu.hk.

^b Laboratory for Synthetic Chemistry and Chemical Biology Limited, Units 1503-1511, 15/F, Building 17 W, Hong Kong Science Park, New Territories, Hong Kong, P. R. China.

^c State Key Laboratory of Terahertz and Millimetre Waves, City University of Hong Kong, Tat Chee Avenue, Kowloon, Hong Kong, P. R. China.

^d State Key Laboratory of Organic Electronics and Information Displays & Jiangsu Key Laboratory for Biosensors, Institute of Advanced Materials (IAM), Nanjing University of Posts and Telecommunications, 9 Wenyuan Road, Nanjing 210023, P. R. China.

Table of Contents

Experimental Section		S7
Scheme S1	Synthetic routes of complexes 1 – 3 . Reaction conditions: (i) 3-(aminomethyl)pyridine, NPC-Tz-NHBoc, TEA, CH ₂ Cl ₂ , rt; (ii) [Re(N [^] N)(CO) ₃ (CH ₃ CN)](CF ₃ SO ₃) (N [^] N = phen, Me ₄ -phen and Ph ₂ -phen), py-Tz-NHBoc, THF, reflux.	S31
Scheme S2	Synthetic routes of complex 4 . Reaction conditions: (i) (1) py-Tz-NHBoc, CH ₂ Cl ₂ /TFA (10:1, v/v), rt; (2) mPEG ₅₀₀₀ -NHS, TEA, CH ₂ Cl ₂ , rt; (ii) [Re(Ph ₂ -phen)(CO) ₃ (CH ₃ CN)](CF ₃ SO ₃), py-Tz-PEG ₅₀₀₀ , THF, reflux.	S31
Table S1	Electronic absorption data of complexes 1 – 4 in CH ₂ Cl ₂ and CH ₃ CN at 298 K.	S32
Table S2	Photophysical data of complexes 1 – 4 .	S33
Table S3	¹ O ₂ generation quantum yields (Φ_{Δ}) of complexes 1 – 4 and their aminomethylpyridine counterparts 1a – 3a in aerated CH ₃ CN at 298 K. DPBF was used as the ¹ O ₂ scavenger and [Ru(bpy) ₃]Cl ₂ was adopted as the reference ($\lambda_{\text{ex}} = 450$ nm).	S34
Table S4	Cellular uptake efficiencies of complexes 1 – 4 towards MDA-MB-231 cells.	S35
Figure S1	Electronic absorption spectra of complexes 1 – 4 in CH ₂ Cl ₂ (black) and CH ₃ CN (red) at 298 K.	S36

Figure S2	Normalised emission spectra of complexes 1 – 4 in CH ₂ Cl ₂ (black) and CH ₃ CN (red) at 298 K and alcohol glass at 77 K (blue).	S37
Figure S3	Pseudo first-order kinetics for the reactions of complexes 1 – 4 with TCO-OH at different concentrations in H ₂ O/DMSO (99:1, v/v) at 298 K. The slope corresponds to the <i>k</i> ₂ of the reaction.	S38
Figure S4	HPLC traces of complexes 1 – 3 (20 μM) treated without (black) or with (red) TCO-OH (200 μM) in H ₂ O/DMSO (99:1, v/v) for 12 h at 298 K.	S39
Figure S5	Release properties of complexes 1 – 4 (20 μM) after incubation with TCO-OH (200 μM) in H ₂ O/DMSO (99:1, v/v) at 298 K.	S40
Figure S6	ESI-mass spectra of the eluates collected at <i>t</i> _R = 1.47, 3.31 and 4.67 min of the reaction of complexes 1 – 3 (20 μM), respectively, with TCO-OH (200 μM) in H ₂ O/DMSO (99:1, v/v).	S41
Figure S7	ESI-mass spectra of the eluates collected at <i>t</i> _R = 2.21 and 3.63 min (complex 1); 3.58 min (complex 2); 5.82 and 6.34 min (complex 3) of the reaction of complexes 1 – 3 (20 μM) with TCO-OH (200 μM) in H ₂ O/DMSO (99:1, v/v).	S42

Figure S8	Emission spectra of complexes 1 – 4 (10 μ M) in the absence (black) and presence (red) of TCO-OH (100 μ M) in H ₂ O/DMSO (99: 1, v/v) upon incubation at 298 K for 12 h.	S43
Figure S9	Rates of decay of absorbance of DPBF (100 μ M) at 410 nm in aerated CH ₃ CN in the presence of complexes 1 – 4 and their aminomethylpyridine counterparts 1a – 3a ($\lambda_{\text{ex}} = 450$ nm).	S44
Figure S10	ESI-mass spectra of a CH ₂ Cl ₂ extract of lysed MDA-MB-231 cells that were pre-treated with TCO-OH (100 μ M, 2 h), followed by incubation with complexes 1 – 4 (10 μ M, 6 h) and fresh medium (12 h).	S45
Figure S11	LSCM images of MDA-MB-231 cells incubated with complex 3a (5 μ M; $\lambda_{\text{ex}} = 405$ nm, $\lambda_{\text{em}} = 500 – 600$ nm) for 6 h, left in fresh medium for 12 h, and then stained with ER-Tracker Green (1 μ M, 15 min; $\lambda_{\text{ex}} = 488$ nm, $\lambda_{\text{em}} = 500 – 520$ nm). Pearson's correlation coefficient = 0.98. Scale bar = 50 μ m.	S46
Figure S12	LSCM images of MDA-MB-231 cells incubated with complex 3a (5 μ M; $\lambda_{\text{ex}} = 405$ nm, $\lambda_{\text{em}} = 500 – 600$ nm) at 37°C (left) or 4°C (right) for 3 h. Scale bar = 50 μ m.	S47
Figure S13	LSCM images of acidic autophagic vacuoles in MDA-MB-231 cells under different conditions. The cells were first pretreated without or with TCO-OH (100 μ M) for 2 h, then	S48

incubated with complex **4** (10 μM) for 6 h, left in fresh medium for 12 h, remained in the dark or irradiated at 450 nm for 20 min (20 mW cm^{-2}), and subsequently incubated in the dark for 2 h. The samples were then stained with MDC (50 μM , 30 min; $\lambda_{\text{ex}} = 488 \text{ nm}$, $\lambda_{\text{em}} = 500 - 520 \text{ nm}$). Scale bar = 50 μm .

Figure S14 LSCM images of (a) CRT (CRT-Alexa 488 (10 μM , 1:200 solution, 2 h; $\lambda_{\text{ex}} = 488 \text{ nm}$, $\lambda_{\text{em}} = 500 - 520 \text{ nm}$); Hoechst 33258 (10 μM , 1 $\mu\text{g mL}^{-1}$, 10 min; $\lambda_{\text{ex}} = 405 \text{ nm}$, $\lambda_{\text{em}} = 420 - 450 \text{ nm}$)) and (b) HMGB1 (HMGB1-Alexa 488 (10 μM , 1:200 solution, 2 h; $\lambda_{\text{ex}} = 488 \text{ nm}$, $\lambda_{\text{em}} = 500 - 520 \text{ nm}$); Hoechst 33258 (10 μM , 1 $\mu\text{g mL}^{-1}$, 10 min; $\lambda_{\text{ex}} = 405 \text{ nm}$, $\lambda_{\text{em}} = 420 - 450 \text{ nm}$)). The cells were treated with complex **3a** (5 μM) for 6 h, left in fresh medium for 12 h, remained in the dark or were irradiated at 450 nm (20 mW cm^{-2}) for 20 min, and subsequently incubated in the dark for 2 h. Scale bar = 25 μm . S49

Figure S15 Extracellular ATP concentrations of MDA-MB-231 cells under different treatments. The cells were treated with complex **3a** (5 μM) for 6 h, left in fresh medium for 12 h, remained in the dark or were irradiated at 450 nm (20 mW S50

cm⁻²) for 20 min, and subsequently incubated in the dark for 2 h.

Figure S16	¹ H NMR spectrum of py-Tz-NHBoc in CDCl ₃ at 298 K.	S51
Figure S17	¹ H NMR spectrum of py-Tz-PEG ₅₀₀₀ in CDCl ₃ at 298 K.	S52
Figure S18	MALDI-TOF mass spectrum of py-Tz-PEG ₅₀₀₀ .	S53
Figure S19	¹ H NMR spectrum of complex 1 in CDCl ₃ at 298 K.	S54
Figure S20	¹³ C NMR spectrum of complex 1 in CDCl ₃ at 298 K.	S55
Figure S21	HR-ESI-mass spectrum of complex 1 in MeOH.	S56
Figure S22	¹ H NMR spectrum of complex 2 in CDCl ₃ at 298 K.	S57
Figure S23	¹³ C NMR spectrum of complex 2 in CDCl ₃ at 298 K.	S58
Figure S24	HR-ESI-mass spectrum of complex 2 in MeOH.	S59
Figure S25	¹ H NMR spectrum of complex 3 in CDCl ₃ at 298 K.	S60
Figure S26	¹³ C NMR spectrum of complex 3 in CDCl ₃ at 298 K.	S61
Figure S27	HR-ESI-mass spectrum of complex 3 in MeOH.	S62
Figure S28	¹ H NMR spectrum of complex 4 in CDCl ₃ at 298 K.	S63
Figure S29	MALDI-TOF mass spectrum of complex 4 .	S64
References		S65

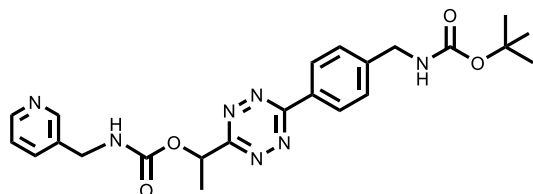
Experimental Section

Materials and Synthesis

All solvents were of analytical grade and purified according to standard procedures.¹ Methoxy poly(ethylene glycol) succinimidyl carboxymethyl ester (mPEG₅₀₀₀-NHS) was purchased from JenKem Technology Co. Ltd. Ammonium chloride (NH₄Cl), oligomycin, chloroquine phosphate, tetraethylammonium chloride, and 2-deoxy-D-glucose were purchased from Sigma Aldrich. Silver trifluoromethanesulfonate, trifluoroacetic acid (TFA), triethylamine (TEA), NH₄OH, magnesium sulfate, 3-(aminomethyl)pyridine, 3-(4,5-dimethyl-2-thiazolyl)-2,5-diphenyltetrazolium bromide (MTT), Re(CO)₅Br, 1,10-phenanthroline (phen), 3,4,7,8-tetramethyl-1,10-phenanthroline (Me₄-phen), 4,7-diphenyl-1,10-phenanthroline (Ph₂-phen), and 1,3-diphenylisobenzofuran (DPBF) were purchased from Acros. *trans*-Cyclooct-4-en-1-ol (TCO-OH) was purchased from BroadPharm. Primary antibodies of HMGB1, CALR, LC3B, SQSTM1 (p62), β-Actin, and secondary antibody IgG(8A3)/HRP were purchased from Solarbio. Autophagy staining assay kit with MDC, Alexa Fluor 488-labeled goat anti-rabbit IgG(H+L), Hoechst 33258, Calcein-AM, ATP assay kit, and propidium iodide (PI) were obtained from Beyotime. Cathepsin B assay kit (Magic Red) was received from Abcam. ELISA MAX™ standard set human TNF-α, Alexa Fluor® 647 anti-human CD80 antibody, FITC anti-human CD86 antibody, FITC anti-human CD3 antibody, and Alexa Fluor® 647 anti-human CD8 antibody were obtained from Biolegend. *tert*-Butyl 4-(6-(1-(((4-nitrophenoxy)carbonyl)oxy)ethyl)-1,2,4,5-tetrazin-3-yl)benzylcarbamate (NPC-Tz-NHBoc)² and the rhenium(I) complexes [Re(N[^]N)(CO)₃(L)](CF₃SO₃) (N[^]N = phen, Me₄-

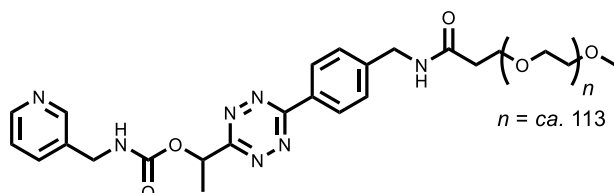
phen, and Ph₂-phen; L = CH₃CN and 3-(aminomethyl)pyridine)³ were prepared according to the literature procedures. All buffer components were of biological grade and used as received. Dulbecco's modified Eagle's medium (DMEM), Roswell Park Memorial Institute (RPMI) 1640, phosphate-buffered saline (PBS), fetal bovine serum (FBS), penicillin/streptomycin, trypsin-EDTA, LysoTracker Deep Red, acridine orange, annexin V/PI assays, and CM-H₂DCFDA were purchased from Invitrogen. Autoclaved Milli-Q water was used for the preparation of the aqueous solutions. MDA-MB-231, NCI-H460, and HepG2 cells were obtained from American Type Culture Collection. Human peripheral blood mononuclear cells (HPBMCs) were purchased from STEMCELL Technologies. The growth medium for cell culture contained DMEM or RPMI 1640 with 10 % FBS and 1 % penicillin/streptomycin.

3-(1-(6-(4-(*N*-Boc-aminomethyl)-phenyl)-1,2,4,5-tetrazin-3-yl)ethyloxycarbonyl-aminomethyl)pyridine (py-Tz-NHBoc)



A mixture of *NPC-Tz-NHBoc*² (200 mg, 0.4 mmol) and 3-(aminomethyl)pyridine (120 μ L, 1.2 mmol) and TEA (700 μ L, 2 mmol) in dry CH_2Cl_2 (20 mL) was stirred at room temperature under an inert atmosphere of nitrogen for 12 h. The solvent was evaporated to yield a purple solid, which was purified by column chromatography on silica gel using $\text{CH}_2\text{Cl}_2/\text{MeOH}$ (50:1, v/v) as the eluent. The solvent was removed under reduced pressure to give a purple solid. Yield: 111 mg (60%). ¹H NMR (300 MHz, CDCl_3 , 298 K, TMS) δ = 8.61 – 8.55 (m, 4H, H2 and H6 of pyridine, and H2 and H6 of phenyl ring), 7.69 (d, 1H, J = 7.8 Hz, H4 of pyridine) 7.55 (d, 2H, J = 8.4 Hz, H3 and H5 of phenyl ring), 7.31 (d, 1H, J = 6.8 Hz, H5 of pyridine), 6.34 – 6.27 (m, 1H, CHCH_3), 5.46 (t, 1H, J = 6.0 Hz, py- CH_2NH), 5.02 (br, 1H, Ph- CH_2NH), 4.47 – 4.40 (m, 4H, CH_2 of pyridine ring and CH_2 of phenyl ring), 1.87 (d, 3H, J = 6.9 Hz, CHCH_3), 1.51 (s, 9H, CH_3 of Boc). MS (ESI, positive-ion mode): m/z 465 [$\text{M} + \text{H}^+$]⁺.

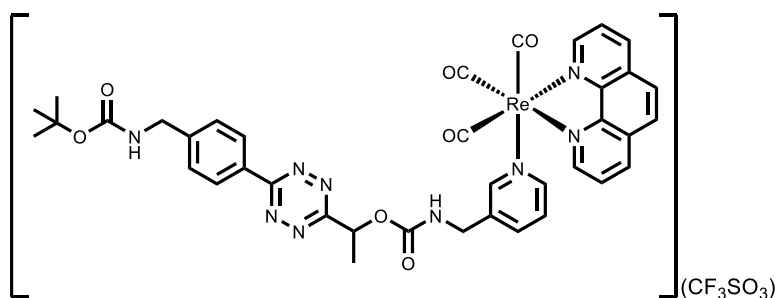
3-(1-(6-(4-(*N*-(3-(ω -methoxypoly(1-oxapropyl))-propanoyl)-aminomethyl)-phenyl)-1,2,4,5-tetrazin-3-yl)ethyloxycarbonylaminoethyl)pyridine (py-Tz-PEG₅₀₀₀)



A mixture of py-Tz-NHBoc (100 mg, 0.21 mmol) and TFA (2 mL) in CH₂Cl₂ (20 mL) was stirred at room temperature under an inert atmosphere of nitrogen for 2 h. The solution was neutralised by the addition of NH₄OH. The mixture was extracted with CH₂Cl₂ (100 mL \times 2), and the organic extract was washed with H₂O (100 mL \times 3). The combined organic extract was dried over MgSO₄, filtered, and the solvent was removed by rotary evaporation to give a purple solid (py-Tz-NH₂). The crude solid was dissolved in dry CH₂Cl₂ (20 mL), and mPEG₅₀₀₀-NHS (410 mg, 0.08 mmol) and TEA (55 μ L, 0.4 mmol) were added. The mixture was stirred at room temperature under an inert atmosphere of nitrogen for 12 h. The solvent was evaporated to yield a purple solid, which was purified by column chromatography on silica gel using CH₂Cl₂/MeOH (10:1, v/v) as the eluent. The solvent was removed under reduced pressure to give a purple solid. Yield: 345 mg (80%). ¹H NMR (300 MHz, CDCl₃, 298 K) δ = 9.01 (d, 1H, *J* = 6.6 Hz, H6 of pyridine), 8.68 – 8.43 (m, 3H, H2 of pyridine, H2 and H6 of phenyl ring), 7.97 (d, 1H, *J* = 7.8 Hz, H4 of pyridine), 7.71 (d, 1H, *J* = 7.3 Hz, H3 of phenyl ring), 7.57 (d, 1H, *J* = 7.4 Hz, H5 of phenyl ring), 7.39 (d, 1H, *J* = 6.9 Hz, H5 of pyridine), 6.25 (br,

1H, py-CH₂NH), 5.62 (s, 1H, CHCH₃), 5.03 (br, 1H, Ph-CH₂NH), 4.63 – 4.55 (m, 4H, CH₂ of pyridine and CH₂ of phenyl ring), 4.12 (d, 2H, *J* = 11.3 Hz, NHCOCH₂), 3.83 – 3.48 (m, ~450 H, OCH₂), 3.39 (s, 3H, OCH₃), 1.89 – 1.76 (dd, 3H, *J* = 6.5 and 6.4 Hz, CHCH₃). MALDI-TOF-MS: number average molecular weight (*M_n*) = 5360.95, weight average molecular weight (*M_w*) = 5449.89, PDI = 1.02.

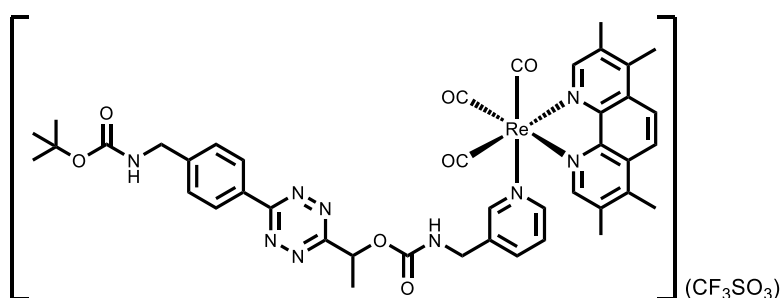
[Re(phen)(CO)₃(py-Tz-NHBoc)](CF₃SO₃) (**1**)



A mixture of [Re(CO)₃(phen)(CH₃CN)](CF₃SO₃)³ (100 mg, 0.20 mmol) and py-Tz-NHBoc (93 mg, 0.2 mmol) in dry THF (20 mL) was refluxed under an inert atmosphere of nitrogen for 12 h. The mixture was evaporated to dryness under reduced pressure to give a purple solid, which was purified by column chromatography on silica gel using CH₂Cl₂/MeOH (25:1, v/v) as the eluent. The solvent was removed under reduced pressure to yield a purple solid. Recrystallisation of the solid from CH₂Cl₂/diethyl ether to afford complex **1** as purple crystals. Yield: 120 mg (60%). ¹H NMR (300 Hz, CDCl₃, 298 K) δ = 9.80 (d, 1H, *J* = 4.9 Hz, H2 of phen), 9.62 (d, 1H, *J* = 4.9 Hz, H9 of phen), 8.83 – 8.75 (m, 2H, H4 and H7 of phen), 8.54 (d, 2H, *J* = 9.0 Hz, H2 and H6 of phenyl ring),

8.27 – 8.10 (m, 5H, H3, H5, H6, and H8 of phen, and H2 of pyridine), 7.66 (d, 1H, $J = 7.5$ Hz, H6 of pyridine), 7.52 (d, 2H, $J = 9.0$ Hz, H3 and H5 of phenyl ring), 7.30 (s, 1H, H4 of pyridine), 7.14 – 7.09 (m, 1H, H5 of pyridine), 6.72 – 6.70 (m, 1H, py-CH₂NH), 6.09 – 6.05 (m, 1H, CHCH₃), 5.09 (br, 1H, Ph-CH₂NH), 4.46 (s, 2H, CH₂ of pyridine), 4.29 – 4.22 (m, 2H, CH₂ of phenyl ring), 1.87 – 1.83 (m, 3H, CHCH₃), 1.49 (s, 9H, CH₃ of Boc).
¹³C NMR (150 MHz, CDCl₃, 298 K) 195.15, 191.01, 169.09, 164.75, 156.26, 156.01, 154.11, 153.63, 150.60, 149.73, 146.59, 146.55, 144.44, 140.64, 140.23, 139.49, 139.19, 138.94, 131.38, 131.24, 130.55, 128.74, 128.45, 128.22, 128.17, 127.52, 127.31, 126.04, 79.90, 71.00, 65.86, 44.40, 41.61, 28.42, 19.96, 15.28. IR (KBr) $\tilde{\nu}/\text{cm}^{-1}$: 2026 (s, C≡O), 1915 (s, C≡O), 1142 (m, CF₃SO₃), 1033 (m, CF₃SO₃). HRMS (ESI, positive-ion mode m/z): [M – CF₃SO₃⁻]⁺ calcd for ReC₃₈H₃₅O₇N₉ 916.2217, found 916.2204.

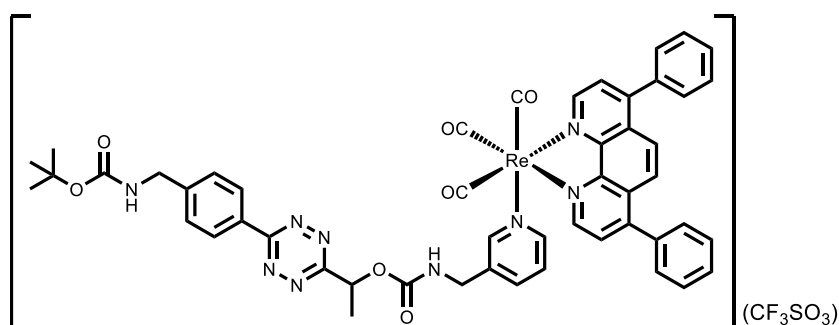
[Re(Me₄-phen)(CO)₃(py-Tz-NHBoc)](CF₃SO₃) (**2**)



The synthetic procedure was similar to that of complex **1**, except that [Re(Me₄-phen)(CO)₃(CH₃CN)](CF₃SO₃) (100 mg, 0.20 mmol) was used instead of [Re(CO)₃(phen)(CH₃CN)](CF₃SO₃). Subsequent recrystallisation of the purple solid from

CH₂Cl₂/diethyl ether afforded complex **2** as purple crystals. Yield: 143 mg (64%). ¹H NMR (600 MHz, CDCl₃, 298 K) δ = 9.44 (s, 1H, H2 of Me₄-phen), 9.21 (s, 1H, H9 of Me₄-phen), 8.61 (d, 2H, *J* = 7.6 Hz, H2 and H6 of phenyl ring), 8.26 – 8.22 (m, 2H, H2 and H6 of pyridine), 8.16 (s, 1H, H5 of Me₄-phen), 8.08 (s, 1H, H6 of Me₄-phen), 7.70 (s, 1H, H4 of pyridine), 7.53 (d, 2H, *J* = 7.9 Hz, H3 and H5 of phenyl ring), 7.15 (s, 1H, H5 of pyridine), 6.72 (br, 1H, py-CH₂NH), 6.16 (d, 1H, *J* = 6.6 Hz, CHCH₃), 5.01 (br, 1H, Ph-CH₂NH), 4.46 (s, 2H, CH₂ of pyridine), 4.30 – 4.16 (m, 2H, CH₂ of phenyl ring), 2.91 – 2.76 (m, 12 H, CH₃ at C3, C4, C7 and C8 of Me₄-phen), 1.86 (d, 3H, *J* = 6.8 Hz, CHCH₃), 1.63 (s, 9H, CH₃ of Boc). ¹³C NMR (150 MHz, CDCl₃, 298 K) 169.12, 164.78, 156.40, 155.97, 153.93, 153.33, 150.32, 149.62, 149.08, 148.52, 145.50, 145.31, 144.29, 143.24, 141.76, 139.14, 138.85, 137.17, 136.59, 135.80, 130.67, 129.99, 129.80, 128.48, 128.16, 126.12, 124.66, 123.90, 121.51, 119.39, 70.87, 65.87, 41.66, 29.71, 28.41, 20.08, 18.14, 17.97, 15.63, 15.55, 15.28. IR (KBr) $\tilde{\nu}$ /cm⁻¹: 2031 (s, C≡O), 1923 (s, C≡O), 1141 (m, CF₃SO₃), 1032 (m, CF₃SO₃). HRMS (ESI, positive-ion mode *m/z*): [M – CF₃SO₃]⁺ calcd for ReC₄₂H₄₃O₇N₉ 972.2843, found 972.2829.

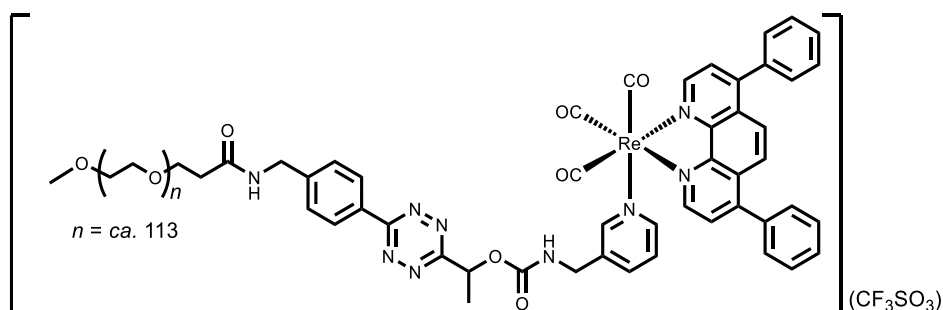
[Re(Ph₂-phen)(CO)₃(py-Tz-NHBoc)](CF₃SO₃) (**3**)



The synthetic procedure was similar to that of complex **1**, except that [Re(Ph₂-phen)(CO)₃(CH₃CN)](CF₃SO₃) (100 mg, 0.20 mmol) was used instead of [Re(CO)₃(phen)(CH₃CN)](CF₃SO₃). Subsequent recrystallisation of the purple solid from CH₂Cl₂/diethyl ether afforded complex **3** as purple crystals. Yield: 133 mg (55%). ¹H NMR (300 MHz, CDCl₃, 298 K) δ = 9.81 (d, 1H, *J* = 4.7 Hz, H2 of Ph₂-phen), 9.61 (d, 1H, *J* = 4.7 Hz, H9 of Ph₂-phen), 8.57 (d, 2H, *J* = 8.2 Hz, H2 and H6 of phenyl ring), 8.34 (s, 2H, H2 and H6 of pyridine), 8.20 (d, 1H, *J* = 4.7 Hz, H3 of Ph₂-phen), 8.16 (s, 2H, H5 and H6 of Ph₂-phen), 8.07 (d, 1H, *J* = 4.8 Hz, H8 of Ph₂-phen), 7.65 – 7.60 (m, 11H, C₆H₅ at C4 and C7 of Ph₂-phen, and H4 of pyridine), 7.52 (d, 2H, *J* = 8.2 Hz, H3 and H5 of phenyl ring), 7.21 (s, 1H, H5 of pyridine), 6.73 (br, 1H, py-CH₂NH), 6.03 – 5.96 (m, 1H, CHCH₃), 5.02 (br, 1H, Ph-CH₂NH), 4.49 (d, 2H, *J* = 4.2 Hz, CH₂ of pyridine), 4.40 – 4.17 (m, 2H, CH₂ of phenyl ring), 1.66 (s, 12H, CHCH₃ and CH₃ of Boc). ¹³C NMR (150 MHz, CDCl₃, 298 K) 195.65, 195.35, 169.14, 164.69, 156.29, 155.96, 153.33, 153.15, 153.01, 152.77, 150.79, 150.03, 147.61, 147.53, 144.29, 143.23, 139.82, 139.00, 135.21, 135.06, 130.63, 130.21, 130.13, 130.01, 129.80, 129.63, 129.25, 129.21, 128.49, 128.21,

127.78, 127.22, 126.62, 126.40, 126.17, 121.48, 119.36, 70.95, 44.40, 41.87, 34.46, 29.70, 28.41, 24.11, 22.69, 19.70. IR (KBr) $\tilde{\nu}/\text{cm}^{-1}$: 2030 (s, C \equiv O), 1920 (s, C \equiv O), 1145 (m, CF₃SO₃), 1030 (m, CF₃SO₃). HRMS (ESI, positive-ion mode m/z): [M – CF₃SO₃⁻]⁺ calcd for ReC₅₀H₄₃O₇N₉ 1068.2843, found 1068.2834.

[Re(Ph₂-phen)(CO)₃(py-Tz-PEG₅₀₀₀)](CF₃SO₃) (**4**)



The synthetic procedure was similar to that of complex **3**, except that py-Tz-PEG₅₀₀₀ (100 mg, 0.20 mmol) was used instead of py-Tz-NHBoc. Subsequent recrystallisation of the purple solid from CH₂Cl₂/diethyl ether afforded complex **4** as purple crystals. Yield: 480 mg (40%). ¹H NMR (400 Hz, CDCl₃, 298 K) δ = 9.82 (s, 1H, H2 of Ph₂-phen), 9.64 (s, 1H, H9 of Ph₂-phen), 8.54 (d, 2H, J = 8.2 Hz, H2 and H6 of phenyl ring), 8.36 (d, 2H, J = 11.6 Hz, H2 and H6 of pyridine), 8.20 – 8.09 (m, 4H, H3, H5, H6, and H8 of Ph₂-phen), 7.65 – 7.55 (m, 13H, C₆H₅ at C4 and C7 of Ph₂-phen, H3 and H5 of phenyl ring), 7.35 (d, 1H, J = 7.1 Hz, H5 of pyridine), 5.98 (d, J = 6.0 Hz, 1H, CHCH₃), 4.63 (d, 2H, J = 5.6 Hz, CH₂ of pyridine), 4.53 (d, 2H, J = 5.1 Hz, CH₂ of phenyl ring), 4.14 (d, 2H, J = 10.8 Hz, NHCOCH₂), 3.83 – 3.48 (m, ~450H, OCH₂), 3.39 (s, 3H, OCH₃), 1.66 (d, 3H, J = 6.9

Hz, CHCH₃). IR (KBr) $\tilde{\nu}/\text{cm}^{-1}$: 2028 (s, C \equiv O), 1917 (s, C \equiv O), 1149 (m, CF₃SO₃), 1027 (m, CF₃SO₃). MALDI-TOF-MS: $M_n = 5981.47$, $M_w = 6065.07$, PDI = 1.01.

Instrumentation and Methods

^1H NMR spectra were recorded on a Bruker 300, 400, or 600 MHz AVANCE III spectrometer at 298 K using deuterated solvents. Chemical shifts (δ , ppm) were reported relative to tetramethylsilane (TMS). Positive-ion ESI mass spectra were recorded on a Perkin-Elmer Sciex API 3200MD mass spectrometer. High-resolution electrospray ionisation (HR-ESI) mass spectra were recorded on a Bruker micrOTOF-QII. MALDI-TOF mass spectra of the samples were recorded on an Applied Biosystems 4800 Plus MALDI TOF/TOFTM Analyser. IR spectra of samples in potassium bromide (KBr) pellets were obtained using a Thermo Scientific Nicolet iS50 FTIR spectrometer in the range of 4000 – 400 cm^{-1} . Electronic absorption and steady-state emission spectra were obtained from an Agilent 8453 diode array spectrophotometer and HORIBA FluoroMax-4 spectrofluorometer, respectively. Luminescence quantum yields were measured by the optically diluted method⁴ using degassed $[\text{Re}(\text{phen})(\text{CO})_3(\text{pyridine})](\text{CF}_3\text{SO}_3)$ ($\Phi_{\text{em}} = 0.18$, $\lambda_{\text{ex}} = 355$ nm) as the standard solution.⁵ Emission lifetimes were measured on an Edinburgh Instruments LP920 laser flash photolysis spectrometer using the third harmonic output (355 nm; 6 – 8 ns fwhm pulse width) of a Spectra-Physics Quanta-Ray Q-switched LAB-150 pulsed S11 Nd:YAG laser (10 Hz) as the excitation source. Unless otherwise specified, all the solutions prepared for photophysical studies were degassed with at least four successive freeze-pump-thaw cycles and stored in a 10- cm^3 round-bottomed flask equipped with a sidearm 1-cm fluorescence cuvette and sealed from the atmosphere by a Rotaflo HP6/6 quick-release Teflon stopper. The dynamical light scattering (DLS) methodology followed the

recommendations outlined in the NIST-protocol.⁶ High-performance liquid chromatography (HPLC) was performed on an Agilent 1260 Infinity II system coupled with a diode array detector WR using H₂O containing 0.1% (v/v) TFA (solvent A) and CH₃CN containing 0.1% (v/v) TFA (solvent B) as the solvents. The diode array detector was set at 220 and 355 nm.

Kinetic Studies

The reaction kinetics of the complexes (10 μM) with TCO-OH (100 – 500 μM) in H₂O/DMSO (99:1, v/v) at 298 K were measured by electronic absorption spectroscopy. The reactions were monitored by following the exponential decay of the absorbance at *ca.* 306 nm upon addition of TCO-OH. Data were fitted to a single-exponential equation to give the pseudo-first-order rate constants k_{obs} , which were then plotted against the concentrations of TCO-OH to obtain the second-order rate constants (k_2) as the slopes of the plots.

Determination of Singlet Oxygen (¹O₂) Generation Quantum Yields (Φ_{Δ})

An aerated CH₃CN solution (2 mL) containing the rhenium(I) complexes and DPBF (10 μM) was introduced to a 1-cm path length quartz cuvette and irradiated with the 450 nm output of a HORIBA Jobin Yvon FluoroMax-4 spectrofluorometer as an excitation source. [Ru(bpy)₃]Cl₂ was used as a reference for ¹O₂ sensitisation ($\Phi_{\Delta} = 0.57$).⁷ The absorbance of the complexes at 450 nm was adjusted to about 0.15. The absorbance of DPBF at 410 nm was monitored every 10 s. A CH₃CN solution of DPBF without the

complexes was examined to determine its photostability under identical irradiation conditions. The Φ_{Δ} of the complexes was determined by comparing Φ_{Δ} of the rhenium(I)-sensitised DPBF photooxidation to Φ_{Δ} of [Ru(bpy)₃]Cl₂-sensitised DPBF photooxidation (as reference) and calculated by the following equation:

$$\Phi_{\Delta}^{unknown} = \Phi_{\Delta}^{reference} \times \frac{m^{unknown} \times F^{reference}}{m^{reference} \times F^{unknown}}$$

where m is the slope of a linear fit of the change of absorbance at 410 nm against the irradiation time and F is the absorption correction factor, which is given as $F = 1 - 10^{-AL}$ (A = absorbance at 450 nm and L = path length of the cuvette).

Transmission Electron Microscopy (TEM)

The diluted complex **4** (20 μ L, 20 μ M) treated with or without TCO-OH (200 μ M) in H₂O/DMSO (99:1, v/v) was deposited onto a carbon-coated copper grid for 30 seconds and the excess solution was removed. The sample grid was left to dry at room temperature for 3 h prior to imaging. Bright-field TEM imaging was performed on a FEI Tecnai12 BioTWIN Transmission Electron Microscope operated at an acceleration voltage of 100 kV. All the TEM images were recorded by a 16 bit 2K \times 2K FEI Eagle bottom mount camera.

Cell Cultures

MDA-MB-231 and HepG2 cells were cultured in DMEM containing 10% FBS and 1% penicillin/streptomycin in an incubator at 37°C under a 5% CO₂ atmosphere. NCI-H460 and HPBMC cells were cultured in RPMI 1640 with 10% FBS and 1% penicillin/streptomycin at 37°C under a 5% CO₂ atmosphere. The cells were subcultured every 2 – 3 days.

Determination of Cellular Uptake by Inductively Coupled Plasma-Mass Spectrometry (ICP-MS)

MDA-MB-231 cells in growth medium were grown in a 50-mm tissue culture dish and incubated at 37°C under a 5% CO₂ atmosphere for 48 h. The culture medium was removed and replaced with a fresh medium containing the rhenium(I) complexes (10 μM). After incubation at 37°C under a 5% CO₂ atmosphere for 6 h, the medium was removed, and the cell layer was washed gently with PBS (1 mL × 3). The cell layer was then trypsinised and 1 mL of the mixture was put in a 1.5-mL Eppendorf centrifuge tube. The cell number was counted with a Logos Biosystems LUNA-II automated cell counter. The harvested cells were digested with 65% HNO₃ (1 mL) at 60°C for 2 h and the rhenium contents were analysed with a PerkinElmer NexION 2000 ICP-MS.

Live-Cell Confocal Imaging

MDA-MB-231 cells in growth medium were seeded on sterilised coverslips in 35-mm tissue culture dishes and grown at 37°C under a 5% CO₂ atmosphere for 48 h. The

growth medium was replaced with either fresh medium or TCO-OH (100 μ M) in medium/DMSO (99:1, v/v) for 2 h. The medium was removed, and the cell layer was gently washed with PBS (1 mL \times 3). The rhenium(I) complexes (10 μ M; λ_{ex} = 405 nm, λ_{em} = 500 – 600 nm) in medium/DMSO (99:1, v/v) were then added to the cells. After incubation for 6 h, the medium was replaced by fresh medium and the cells were further incubated for 12 h. The cells were imaged using a Leica TCS SPE confocal microscope with an oil immersion 63 \times objective after washing with PBS (1 mL \times 3). In costaining experiments, after the treatments, the cells were incubated with LysoTracker Deep Red (100 nM, 15 min; λ_{ex} = 635 nm, λ_{em} = 640 – 660 nm) in the growth medium. The medium was then removed, and the cell layer was gently washed with PBS (1 mL \times 3). The Pearson's correlation coefficient was determined using the programme ImageJ (Version 1.4.3.67).

MTT Assays

MDA-MB-231, HepG2, and NCI-H460 cells in growth medium were seeded in 96-well flat-bottomed microplates (*ca.* 10,000 cells per well) in growth medium (100 μ L) and incubated at 37 $^{\circ}$ C under a 5% CO₂ atmosphere for 48 h. The cells were treated with or without TCO-OH (100 μ M) in medium/DMSO (99:1, v/v) for 2 h. The medium was removed, and the cell layer was gently washed with PBS (1 mL \times 3). The complexes were then added to the cells with concentrations ranging from 10⁻⁷ to 10⁻⁴ M in medium/DMSO (99:1, v/v), and the cells were incubated at 37 $^{\circ}$ C under a 5% CO₂ atmosphere for 6 h and further incubated in fresh medium for 12 h. Wells containing

untreated cells were used as a blank control. Then the medium was replaced by phenol red-free medium. One of the microplates was irradiated at 450 nm (20 mW cm^{-2}) for 20 min in a LED cellular photocytotoxicity irradiator (PURI Materials, ShenZhen, China) and the other microplate was kept in the dark. After the treatment, the culture medium was replaced with fresh medium, and the cells were incubated at 37°C under a 5% CO_2 atmosphere for 24 h. The medium in each well was then replaced with free medium (90 μL) and 10 μL of MTT (5 mg/mL) in PBS was added. The medium was replaced after incubation for 3 h and DMSO (200 μL) was added to each well. The absorbance of the solutions at 570 nm was measured with a BioTek powerwave XS MQX200R microplate spectrophotometer. The IC_{50} values of the complexes were determined from dose dependence of surviving cells after exposure to the complexes.

Annexin V-FITC/PI Double Staining Assay

MDA-MB-231 cells in growth medium were seeded in two 6-well plates and grown at 37°C under a 5% CO_2 atmosphere for 48 h. The growth medium was replaced with either fresh medium or TCO-OH (100 μM) in medium/DMSO (99:1, v/v) for 2 h. The medium was removed, and the cell layer was gently washed with PBS (1 mL \times 3). The cells were then incubated with complex **4** (10 μM) in medium for 6 h and further incubated in fresh medium for 12 h. After the treatment, the cells were irradiated at 450 nm (20 mW cm^{-2}) for 5 min or kept in the dark. After incubation for 2 h, the medium was removed, and the cell layer was washed gently with PBS (1 mL \times 3). The cell layer was then trypsinised and centrifuged at 1,500 rpm for 1 min. The cell pellet

was washed with PBS (1 mL) and subjected to centrifugation. The cells were resuspended in an annexin V binding buffer (100 μ L) in the flow cytometer tubes, followed by the addition of Alexa Fluor 647-annexin V conjugate (5 μ L) and PI (2 μ L, 100 μ g mL⁻¹). The cell suspension was kept in the dark for 15 min. The annexin V binding buffer (400 μ L) was added to the suspension before analysis by flow cytometer (Beckman CytoFLEX). The untreated cultured cells were used as a control group for background correction. The experiments were analysed using the FlowJo V10 software.

Live/Dead Cell Staining Assay

MDA-MB-231 cells in growth medium were seeded on sterilised coverslips in 35-mm tissue culture dishes and grown at 37°C under a 5% CO₂ atmosphere for 48 h. The growth medium was replaced with either fresh medium or TCO-OH (100 μ M) in medium/DMSO (99:1, v/v) for 2 h. The medium was removed, and the cell layer was gently washed with PBS (1 mL \times 3). The cells were then incubated with complex **4** (10 μ M) in medium for 6 h and further incubated in fresh medium for 12 h. After the treatment, the cells were irradiated at 450 nm (20 mW cm⁻²) for 5 min or kept in the dark. Then the cells were stained with Calcein-AM (1 μ M; λ_{ex} = 408 nm, λ_{em} = 500 – 520 nm) and PI (10 μ M; λ_{ex} = 532 nm, λ_{em} = 600 – 650 nm) in medium for 1 h. Then, the cells were washed with PBS (1 mL \times 3) and imaged using a Leica TCS SPE confocal microscope with an oil immersion 63 \times objective.

3D Tumour Spheroid Model Preparation and PDT Efficiency Evaluation

MDA-MB-231 in growth medium (2×10^4 cells/mL) were seeded in two 96-well cell carrier spheroid ultra-low-attachment microplates. Then, the MDA-MB-231 spheroids were grown in the incubator for one week at 37°C under 5% CO₂ (the diameter of tumour spheroids is over 250 µm), and the medium was replaced with fresh medium every 3 days. To evaluate the PDT efficacy of complex **4** towards spheroids, the growth medium was replaced with either fresh medium or TCO-OH (100 µM) in medium/DMSO (99:1, v/v) for 2 h. The medium was removed, and the cell layer was gently washed with PBS (1 mL \times 3). The spheroids were then incubated with complex **4** (10 µM) in medium for 6 h and further incubated in fresh medium for 12 h. After the treatment, the cells were irradiated at 450 nm (20 mW cm^{-2}) for 5 min or kept in the dark. Then the spheroids were further incubated for another 24 h and stained with Calcein-AM (1 µM; $\lambda_{\text{ex}} = 408 \text{ nm}$, $\lambda_{\text{em}} = 500 - 520 \text{ nm}$) and PI (10 µM; $\lambda_{\text{ex}} = 532 \text{ nm}$, $\lambda_{\text{em}} = 600 - 650 \text{ nm}$) in the medium for 1 h and imaged using a Leica TCS SPE confocal microscope with a 10 \times objective.

Intracellular Reactive Oxygen Species (ROS) Generation

MDA-MB-231 cells in growth medium were seeded on sterilised coverslips in 35-mm tissue culture dishes and grown at 37°C under a 5% CO₂ atmosphere for 48 h. The growth medium was replaced with either fresh medium or TCO-OH (100 µM) in medium/DMSO (99:1, v/v) for 2 h. The medium was removed, and the cell layer was gently washed with PBS (1 mL \times 3). The cells were then incubated with complex **4** (10

μM) in medium for 6 h and further incubated in fresh medium for 12 h. After the treatment, the cells were irradiated at 450 nm (20 mW cm^{-2}) for 5 min or kept in the dark. Then the cells were then incubated with CM-H₂DCFDA ($10 \mu\text{M}$; $\lambda_{\text{ex}} = 488 \text{ nm}$, $\lambda_{\text{em}} = 500 - 520 \text{ nm}$) in medium/DMSO (99:1, v/v) for 20 min. After washing with PBS ($1 \text{ mL} \times 3$), the cells were imaged using a Leica TCS SPE confocal microscope with an oil immersion 63 \times objective.

Acridine Orange (AO) Staining

MDA-MB-231 cells in growth medium were seeded on sterilised coverslips in 35-mm tissue culture dishes and grown at 37°C under a 5% CO₂ atmosphere for 48 h. The growth medium was replaced with either fresh medium or TCO-OH ($100 \mu\text{M}$) in medium/DMSO (99:1, v/v) for 2 h. The medium was removed, and the cell layer was gently washed with PBS ($1 \text{ mL} \times 3$). The cells were then incubated with complex **4** ($10 \mu\text{M}$) in medium for 6 h and further incubated in fresh medium for 12 h. After the treatment, the cells were irradiated at 450 nm (20 mW cm^{-2}) for 5 min or kept in the dark. Then the cells were stained with acridine orange ($10 \mu\text{M}$; $\lambda_{\text{ex}} = 488 \text{ nm}$, $\lambda_{\text{em}} = 500 - 520 \text{ nm}$ (green channel) and 610 – 640 nm (red channel)) in medium at 37°C for 30 min. Following washing the cells with PBS ($1 \text{ mL} \times 3$), the cells were imaged using a Leica TCS SPE confocal microscope with an oil immersion 63 \times objective.

Release of Cathepsin B

MDA-MB-231 cells in growth medium were seeded on sterilised coverslips in 35-mm tissue culture dishes and grown at 37°C under a 5% CO₂ atmosphere for 48 h. The growth medium was replaced with either fresh medium or TCO-OH (100 µM) in medium/DMSO (99:1, v/v) for 2 h. The medium was removed, and the cell layer was gently washed with PBS (1 mL × 3). The cells were then incubated with complex **4** (10 µM) in medium for 6 h and further incubated in fresh medium for 12 h. After the treatment, the cells were irradiated at 450 nm (20 mW cm⁻²) for 5 min or kept in the dark. Then the cells were incubated with Magic Red MR-(RR)₂ (1:100; λ_{ex} = 532 nm, λ_{em} = 630 – 650 nm) in medium at 37°C for 1 h. Then the cells were washed with PBS (1 mL × 3) and imaged using a Leica TCS SPE confocal microscope with an oil immersion 63× objective.

Monodansylcadaverine (MDC) Staining Assay

MDA-MB-231 cells in growth medium were seeded on sterilised coverslips in 35-mm tissue culture dishes and grown at 37°C under a 5% CO₂ atmosphere for 48 h. The growth medium was replaced with either fresh medium or TCO-OH (100 µM) in medium/DMSO (99:1, v/v) for 2 h. The medium was removed, and the cell layer was gently washed with PBS (1 mL × 3). The cells were then incubated with complex **4** (10 µM) in medium for 6 h and further incubated in fresh medium for 12 h. After the treatment, the cells were irradiated at 450 nm (20 mW cm⁻²) for 5 min or kept in the dark. Then the cells were stained with MDC (50 µM; λ_{ex} = 408 nm, λ_{em} = 500 – 520 nm)

in medium at 37°C for 30 min. Then the cells were washed with PBS (1 mL × 3) and imaged using a Leica TCS SPE confocal microscope with an oil immersion 63× objective.

Western Blot Analysis

MDA-MB-231 cells in growth medium were seeded in two 6-well plates and grown at 37°C under a 5% CO₂ atmosphere for 48 h. The growth medium was replaced with either fresh medium or TCO-OH (100 μM) in medium/DMSO (99:1, v/v) for 2 h. The medium was removed, and the cell layer was gently washed with PBS (1 mL × 3). The cells were then incubated with complex **4** (10 μM) in medium for 6 h and further incubated in fresh medium for 12 h. After the treatment, the cells were irradiated at 450 nm (20 mW cm⁻²) for 5 min or kept in the dark. After incubation for 2 h, the cells were washed with cold PBS (1 mL × 3), harvested and lysed using lysis buffer on ice. Following centrifugation for the collection of cellular lysates, the concentration of cellular protein was quantified by the BCA protein assay kit. Total protein samples (20 – 25 μg/lane) were separated on an SDS-PAGE in a Tris-Glycine running buffer and blotted on polyvinylidene fluoride (PVDF) membranes. The PVDF membranes were then blocked by BSA (5%) at room temperature for 1 h, followed by incubation with the primary antibody (LC3B (1:2000), p62 (1:2000), or β-actin (1:2000)) at 4°C overnight and the respective secondary antibody conjugated with horseradish peroxidase (1:5000) for 2 h. Detection was performed by using the chemiluminescence procedure (ECL). Equal loading of the proteins in each lane was verified by the intensity of β-actin.

Immunofluorescence Staining

MDA-MB-231 cells in growth medium were seeded on sterilised coverslips in 35-mm tissue culture dishes and grown at 37°C under a 5% CO₂ atmosphere for 48 h. The growth medium was replaced with either fresh medium or TCO-OH (100 µM) in medium/DMSO (99:1, v/v) for 2 h. The medium was removed, and the cell layer was gently washed with PBS (1 mL × 3). The cells were then incubated with complex 4 (10 µM) in medium for 6 h and further incubated in fresh medium for 12 h. After the treatment, the cells were irradiated at 450 nm (20 mW cm⁻²) for 5 min or kept in the dark. After incubation for 2 h, the cells were fixed with paraformaldehyde (4%) in PBS for 10 min, permeabilised with Triton X-100 (0.1%) solution for 5 min, and blocked with BSA (3%) for 1 h. The cells were then incubated with the primary antibody (LC3B (1:500), CARL (1:500) and HMGB1 (1:500)) in PBS at 4°C overnight. After incubation, the cells were thoroughly washed with PBS (1 mL × 3) and further incubated with anti-rabbit Alexa Fluor 488-conjugated secondary antibody (1:1000; $\lambda_{\text{ex}} = 488 \text{ nm}$, $\lambda_{\text{em}} = 500 - 520 \text{ nm}$) in PBS at 37°C for 1 h. The cells were washed with PBS (1 mL × 3) and the nuclei were stained with Hoechst 33258 (1 µg mL⁻¹; $\lambda_{\text{ex}} = 405 \text{ nm}$, $\lambda_{\text{em}} = 420 - 450 \text{ nm}$) for 10 min. After washing with PBS (1 mL × 3), the cells were imaged using a Leica TCS SPE confocal microscope with an oil immersion 63× objective.

ATP Detection

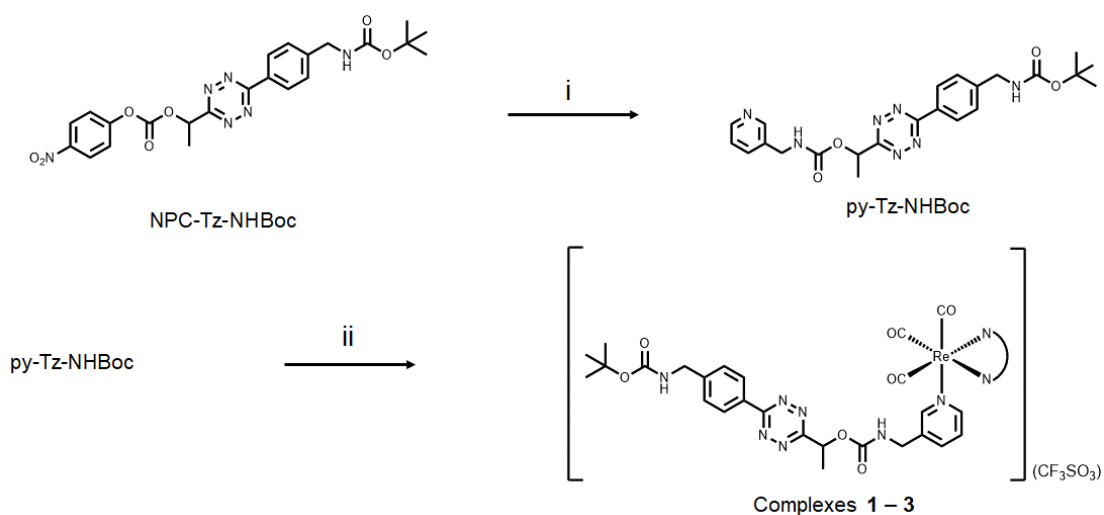
MDA-MB-231 cells in growth medium were seeded in two 96-well flat-bottomed microplates (*ca.* 10,000 cells per well) and incubated at 37°C under a 5% CO₂

atmosphere for 48 h. The cells were pretreated with or without TCO-OH (100 μ M) in medium/DMSO (99:1, v/v) for 2 h. The medium was removed, and the cell layer was gently washed with PBS (1 mL \times 3). The cells were then incubated with complex **4** (10 μ M) in medium/DMSO (99:1, v/v) for 6 h and further incubated in fresh medium for 12 h. After the treatment, the cells were irradiated at 450 nm (20 mW cm⁻²) for 5 min or kept in the dark. Followed by incubation for 2 h, the medium of each sample well (50 μ L) was transferred to a new 96-well flat bottom plate for extracellular ATP measurement by ATP Assay Kit using SPECTRAMax ID5 microplate reader (Molecular Devices Corp., Sunnyvale, CA).

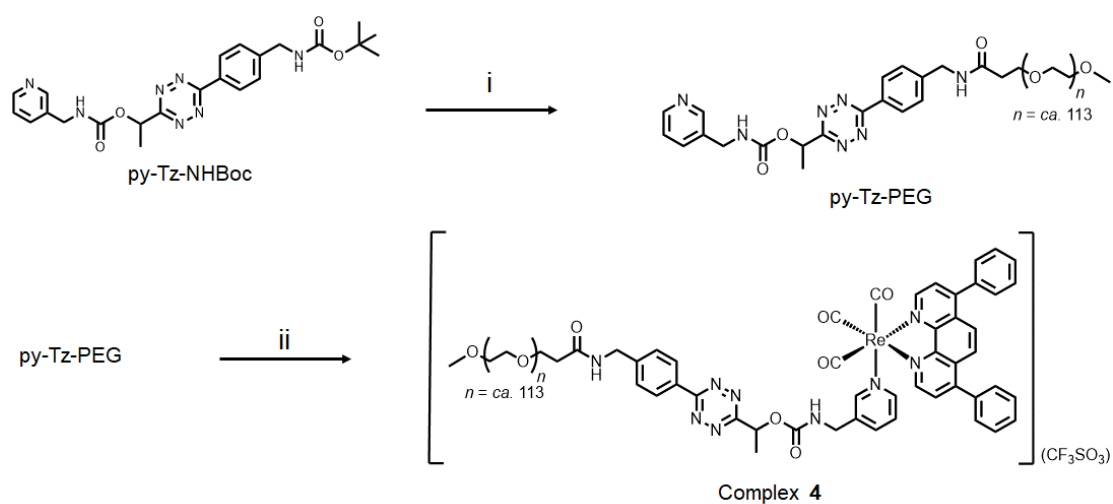
***In Vitro* Dendritic Cell Maturation and T Cell Activation of HPBMCs**

To evaluate the priming of T cells, a transwell cell co-culture model was constructed. Briefly, MDA-MB-231 cells in growth medium were cultured in the upper chamber in 6-well plates and grown at 37°C under a 5% CO₂ atmosphere for 48 h. The growth medium was replaced with either fresh medium or TCO-OH (100 μ M) in medium/DMSO (99:1, v/v) for 2 h. The medium was removed, and the cell layer was gently washed with PBS (1 mL \times 3). The cells were then incubated with complex **4** (10 μ M) in medium for 6 h and further incubated in fresh medium for 24 h. After the treatment, the cells were irradiated at 450 nm (20 mW cm⁻²) for 5 min or kept in the dark. The immature HPBMCs were seeded in the lower compartment and co-cultured with MDA-MB-231 cells for 24 h. Then the HPBMCs were collected and washed with PBS (1 mL \times 2), followed by staining with Alexa Fluor[®] 647 anti-human CD80 antibody

and FITC anti-human CD86 antibody or Alexa Fluor® 647 anti-human CD8 antibody and FITC anti-human CD3 antibody. The cell suspension was kept in the dark at 4°C for 2 h and thoroughly washed with PBS (1 mL × 2). The cells were then resuspended in PBS before analysis by flow cytometer (Beckman CytoFLEX). The experiments were analysed using the FlowJo V10 software. The cytokine IFN- α in suspension were detected by ELISA kits with a standard protocol.



Scheme S1. Synthetic routes of complexes **1 – 3**. Reaction conditions: (i) 3-(aminomethyl)pyridine, NPC-Tz-NHBoc, TEA, CH₂Cl₂, rt; (ii) [Re(N[^]N)(CO)₃(CH₃CN)](CF₃SO₃) (N[^]N = phen, Me₄-phen and Ph₂-phen), py-Tz-NHBoc, THF, reflux.



Scheme S2. Synthetic routes of complex **4**. Reaction conditions: (i) (1) py-Tz-NHBoc, CH₂Cl₂/TFA (10:1, v/v), rt; (2) mPEG₅₀₀₀-NHS, TEA, CH₂Cl₂, rt; (ii) [Re(Ph₂-phen)(CO)₃(CH₃CN)](CF₃SO₃), py-Tz-PEG₅₀₀₀, THF, reflux.

Table S1. Electronic absorption data of complexes **1** – **4** in CH₂Cl₂ and CH₃CN at 298 K.

Complex	Solvent	$\lambda_{\text{abs}}/\text{nm}$ ($\epsilon/\text{dm}^3 \text{ mol}^{-1} \text{ cm}^{-1}$)
1	CH ₂ Cl ₂	262 sh (46,580), 275 (57,430), 331 sh (8,445), 385 sh (4,300), 546 (620)
	CH ₃ CN	263 sh (40,420), 273 (46,930), 328 sh (8,155), 371 sh (3,430), 540 (640)
2	CH ₂ Cl ₂	255 sh (39,555), 287 (57,555), 372 sh (4,420), 530 (670)
	CH ₃ CN	252 sh (33,710), 280 (44,470), 369 sh (3,365), 543 (490)
3	CH ₂ Cl ₂	270 sh (49,440), 287 (56,960), 342 sh (16,980), 397 sh (7,710), 540 (1,105)
	CH ₃ CN	268 sh (33,130), 287 (37,745), 334 sh (11,965), 394 sh (4,420), 535 (770)
4	CH ₂ Cl ₂	267 sh (45,990), 289 (60,650), 341 sh (16,955), 394 sh (7,810), 544 (675)
	CH ₃ CN	264 sh (40,545), 290 (54,365), 337 sh (15,075), 388 sh (6,260), 546 (340)

Table S2. Photophysical data of complexes **1** – **4**.

Complex	Medium (T/K)	λ_{em}/nm	$\tau_0/\mu s$	Φ_{em}
1	CH ₂ Cl ₂ (298)	527	2.23	0.036
	CH ₃ CN (298)	539	1.85	0.030
	Glass ^a (77)	469, 501 sh	6.59	
2	CH ₂ Cl ₂ (298)	513	9.81	0.039
	CH ₃ CN (298)	518	7.40	0.031
	Glas ^a (77)	485 (max), 499, 537	39.17	
3	CH ₂ Cl ₂ (298)	547	8.19	0.030
	CH ₃ CN (298)	559	3.99	0.029
	Glass ^a (77)	510, 529 sh	17.88	
4	CH ₂ Cl ₂ (298)	545	8.85	0.036
	CH ₃ CN (298)	558	4.01	0.032
	Glass ^a (77)	510, 530 sh	18.31	

^a EtOH:MeOH (4:1, v/v)

Table S3. $^1\text{O}_2$ generation quantum yields (Φ_Δ) of complexes **1** – **4** and their aminomethylpyridine counterparts **1a** – **3a** in aerated CH_3CN at 298 K. DPBF was used as a $^1\text{O}_2$ scavenger and $[\text{Ru}(\text{bpy})_3]\text{Cl}_2$ was adopted as a reference ($\lambda_{\text{ex}} = 450 \text{ nm}$).

Complex	Φ_Δ
1	0.22
2	0.25
3	0.48
4	0.27
1a	0.26
2a	0.32
3a	0.63

Table S4. Cellular uptake efficiencies of complexes **1 – 4** towards MDA-MB-231 cells.

Complex	Amount of rhenium/fmol ^a
1	0.32 ± 0.02
2	0.79 ± 0.03
3	1.89 ± 0.03
4	0.28 ± 0.02

^a Amount of rhenium associated with an average MDA-MB-231 cell upon incubation with the rhenium(I) complexes (10 μM) at 37°C for 6 h, as determined by ICP-MS.

Figure S1. Electronic absorption spectra of complexes **1** – **4** in CH_2Cl_2 (black) and CH_3CN (red) at 298 K.

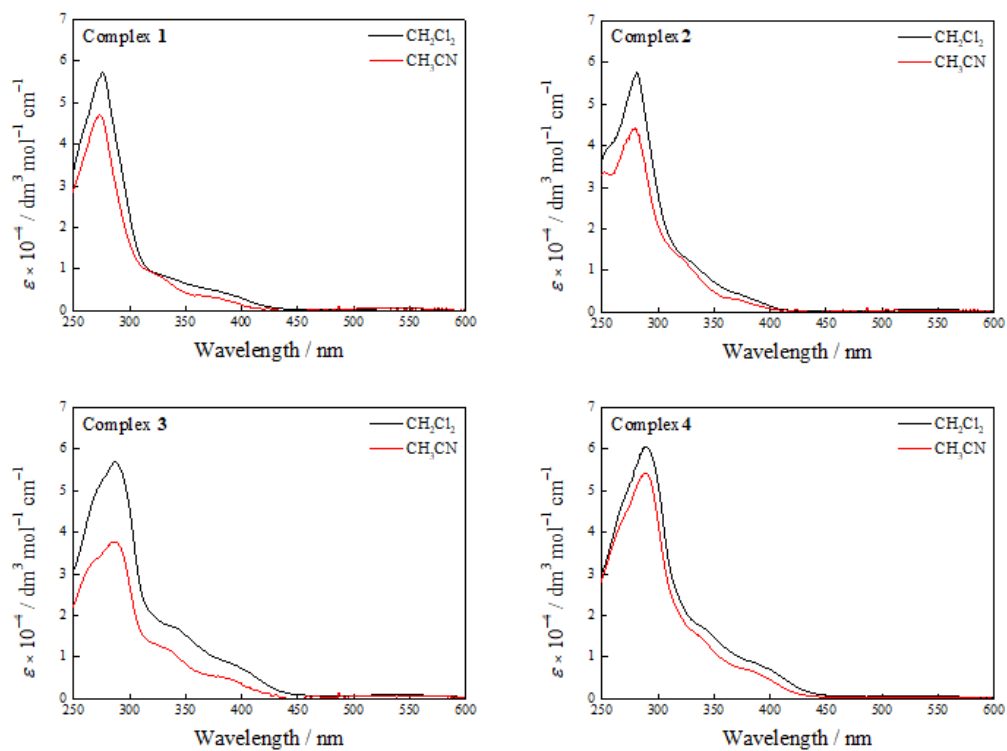


Figure S2. Normalised emission spectra of complexes **1 – 4** in CH_2Cl_2 (black) and CH_3CN (red) at 298 K and alcohol glass at 77 K (blue).

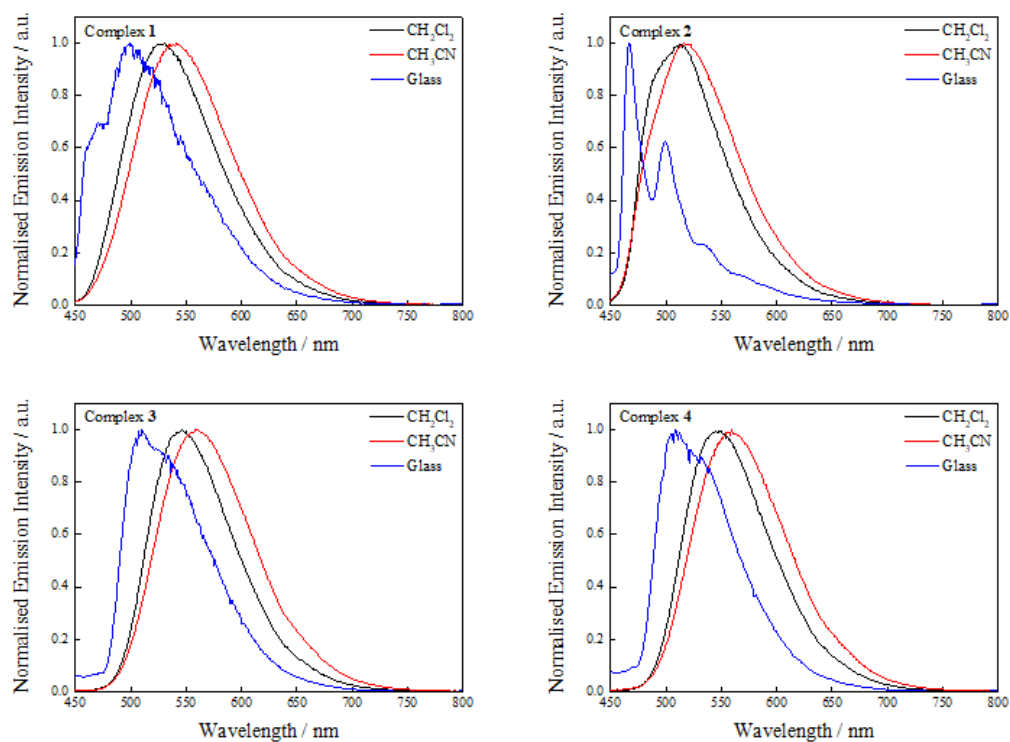


Figure S3. Pseudo first-order kinetics for the reactions of complexes **1** – **4** with TCO-OH at different concentrations in H₂O/DMSO (99:1, v/v) at 298 K. The slope corresponds to the k_2 of the reaction.

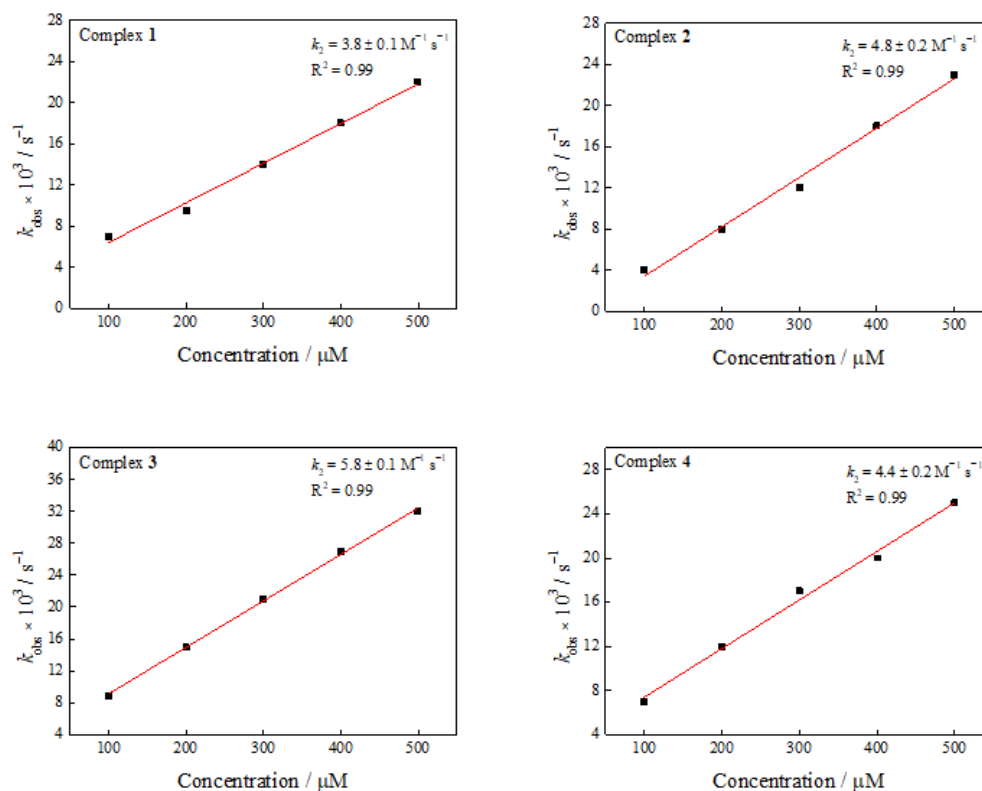


Figure S4. HPLC traces of complexes **1 – 3** (20 μM) treated without (black) or with (red)

TCO-OH (200 μM) in $\text{H}_2\text{O}/\text{DMSO}$ (99:1, v/v) for 12 h at 298 K.

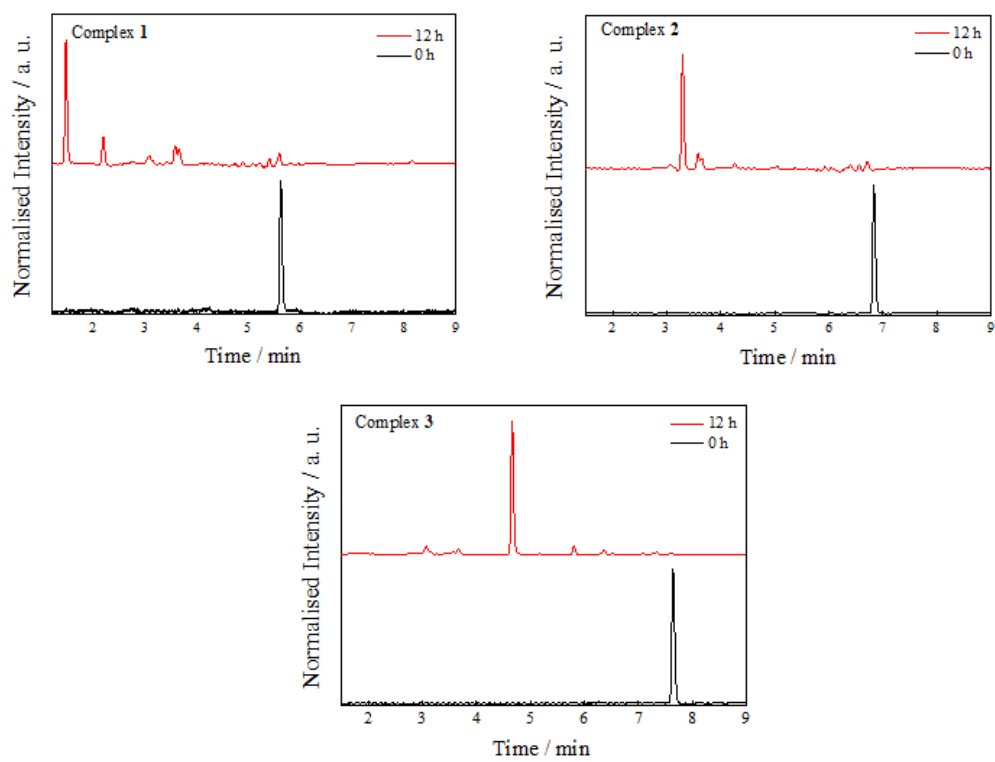


Figure S5. Release properties of complexes **1 – 4** (20 μM) after incubation with TCO-OH (200 μM) in $\text{H}_2\text{O}/\text{DMSO}$ (99:1, v/v) at 298 K.

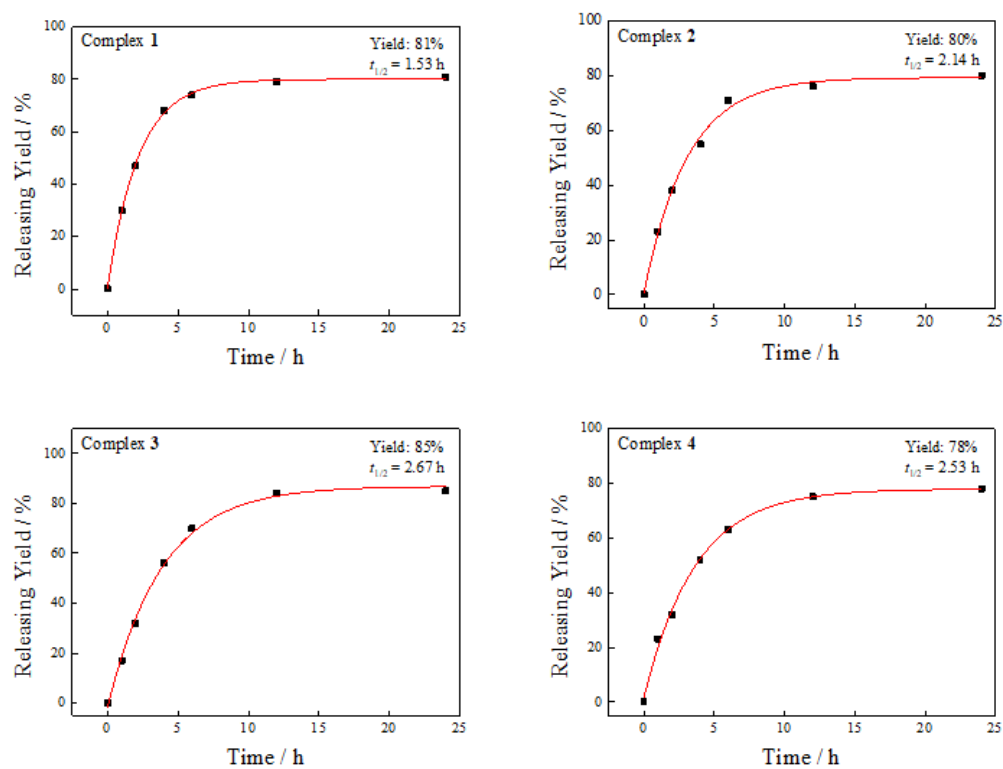


Figure S6. ESI-mass spectra of the eluates collected at $t_R = 1.47, 3.31$ and 4.67 min of the reaction of complexes **1** – **3** ($20 \mu\text{M}$), respectively, with TCO-OH ($200 \mu\text{M}$) in $\text{H}_2\text{O}/\text{DMSO}$ ($99:1, v/v$).

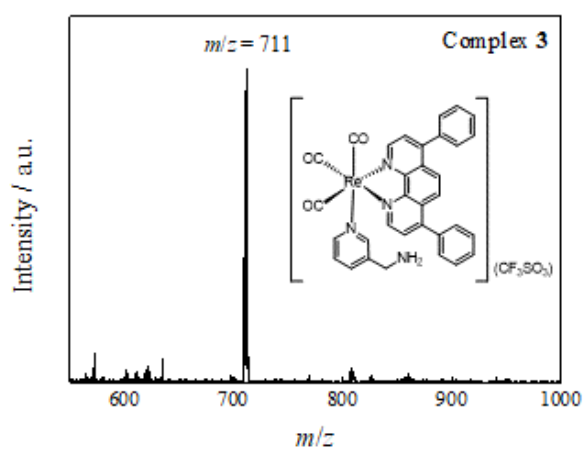
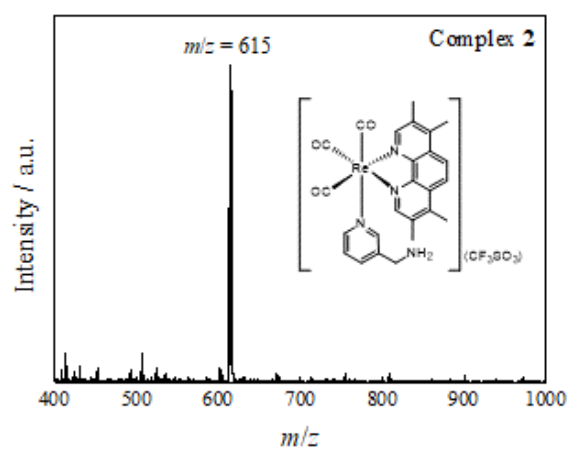
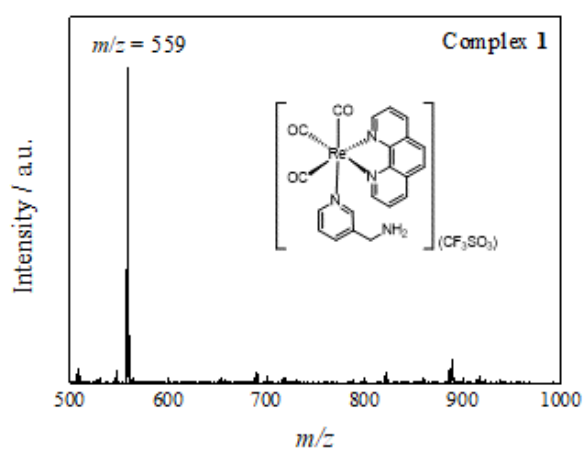


Figure S7. ESI-mass spectra of the eluates collected at $t_R = 2.21$ and 3.63 min (complex **1**); 3.58 min (complex **2**); 5.82 and 6.34 min (complex **3**) of the reaction of complexes **1** – **3** ($20 \mu\text{M}$) with TCO-OH ($200 \mu\text{M}$) in $\text{H}_2\text{O}/\text{DMSO}$ ($99:1, v/v$).

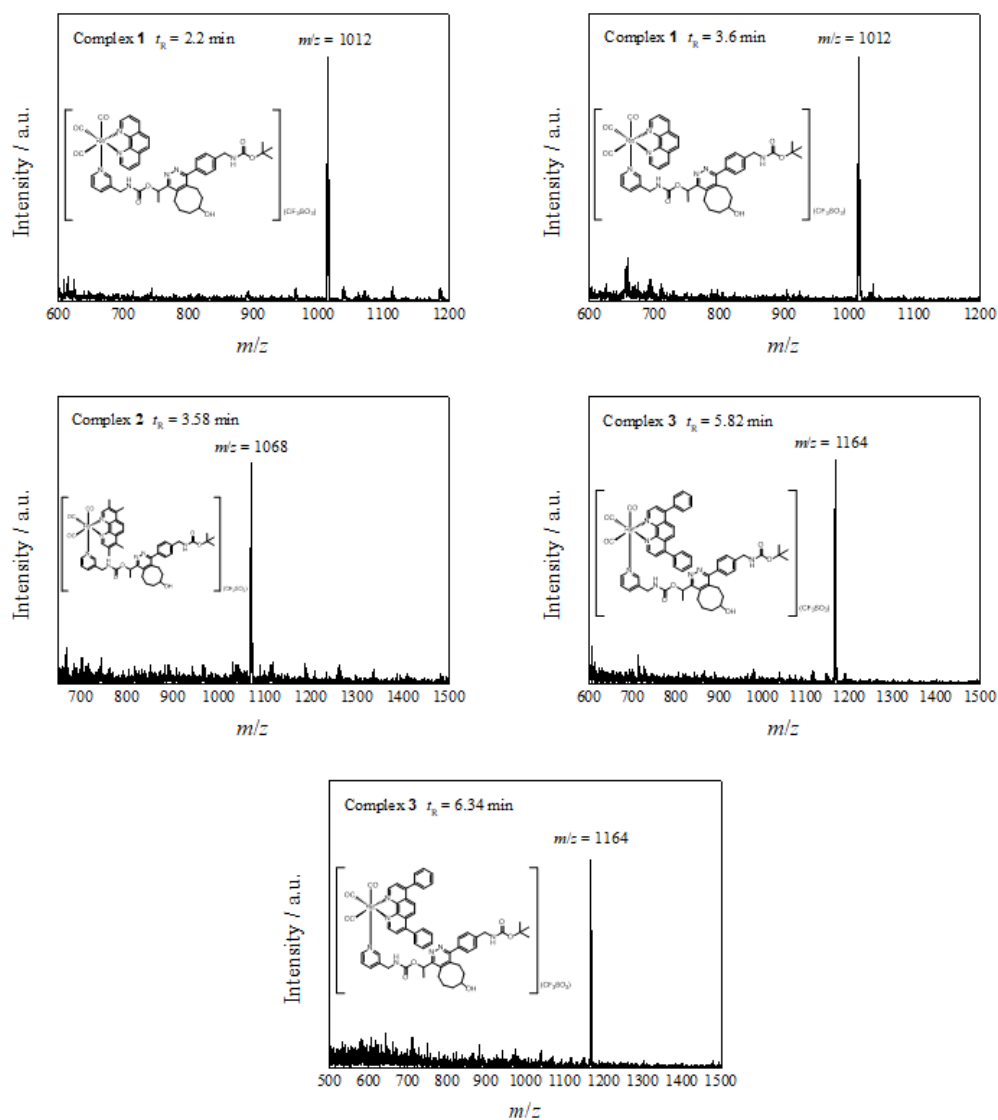


Figure S8. Emission spectra of complexes **1** – **4** (10 μM) in the absence (black) and presence (red) of TCO-OH (100 μM) in $\text{H}_2\text{O}/\text{DMSO}$ (99: 1, v/v) upon incubation at 298 K for 12 h.

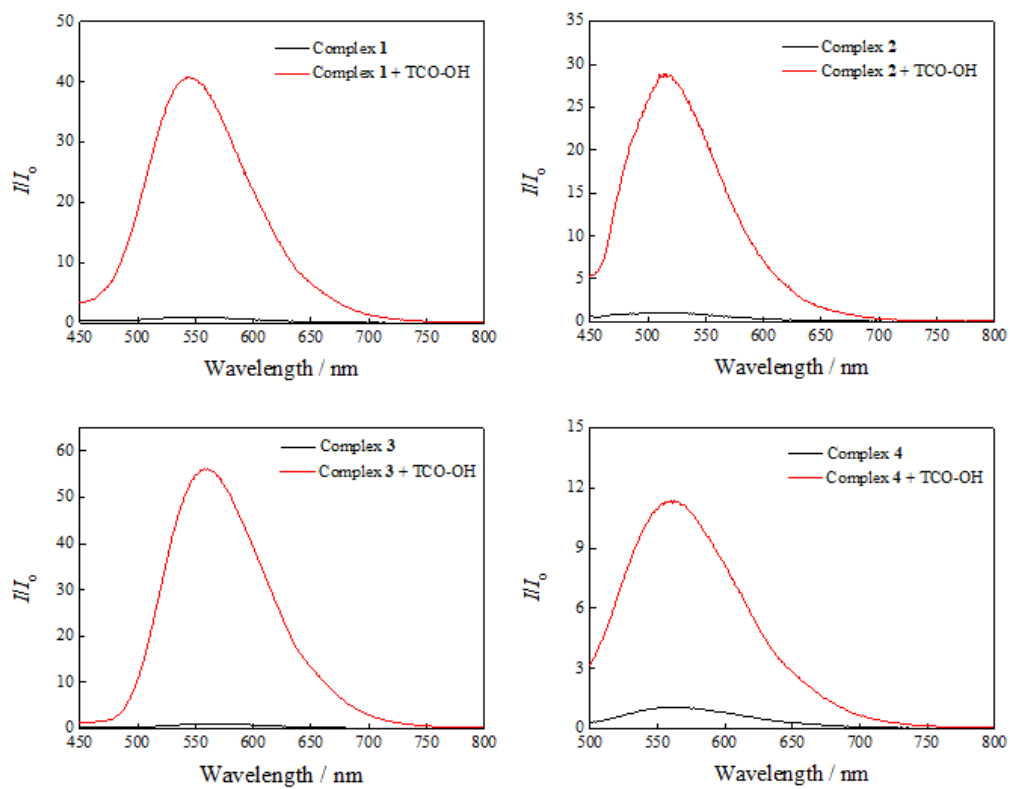


Figure S9. Rates of decay of absorbance of DPBF (100 μ M) at 410 nm in aerated CH_3CN in the presence of complexes **1** – **4** and their aminomethylpyridine counterparts **1a** – **3a** ($\lambda_{\text{ex}} = 450$ nm).

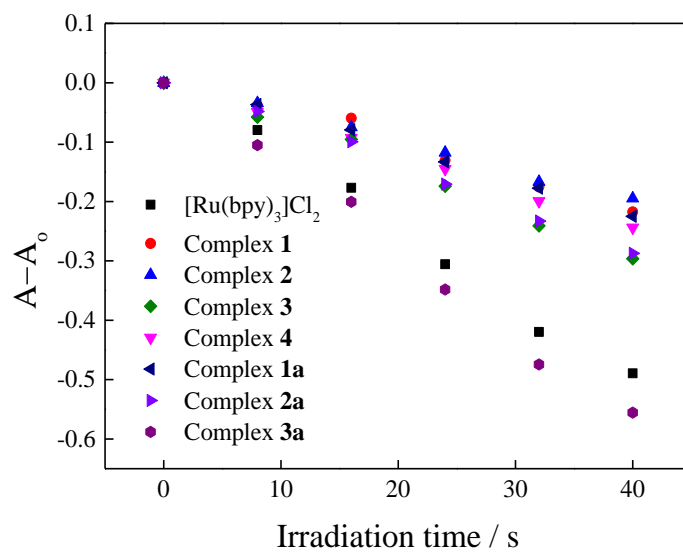


Figure S10. ESI-mass spectra of a CH₂Cl₂ extract of lysed MDA-MB-231 cells that were pre-treated with TCO-OH (100 μM, 2 h), followed by incubation with complexes **1** – **4** (10 μM, 6 h) and fresh medium (12 h).

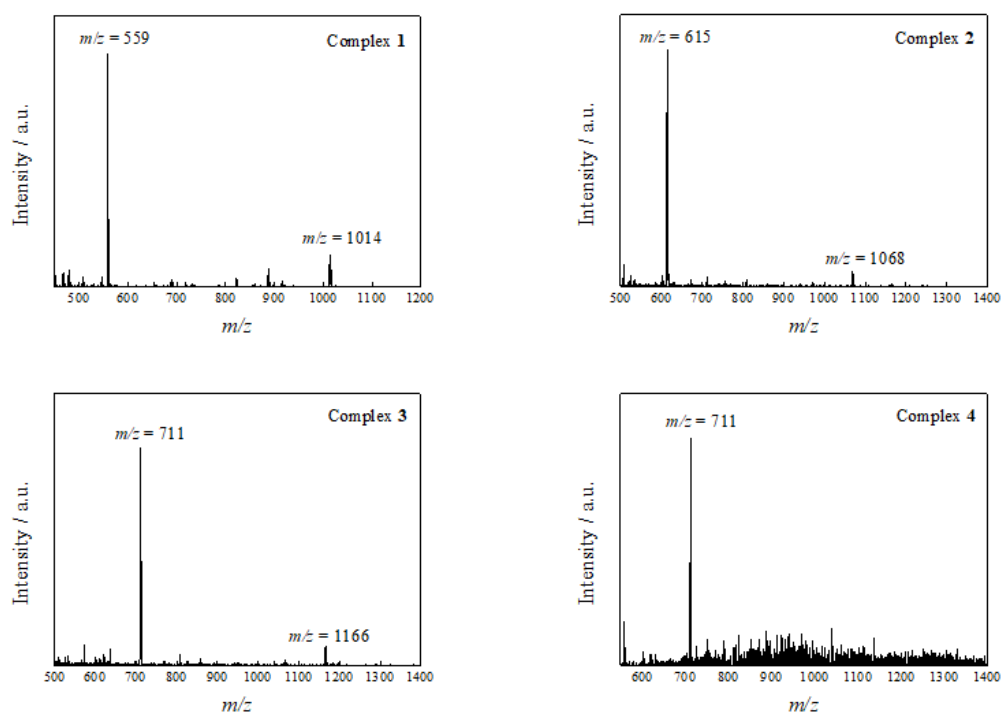


Figure S11. LSCM images of MDA-MB-231 cells incubated with complex **3a** (5 μM ; λ_{ex} = 405 nm, λ_{em} = 500 – 600 nm) for 6 h, left in fresh medium for 12 h, and then stained with ER-Tracker Green (1 μM , 15 min; λ_{ex} = 488 nm, λ_{em} = 500 – 520 nm). Pearson's correlation coefficient = 0.98. Scale bar = 50 μm .

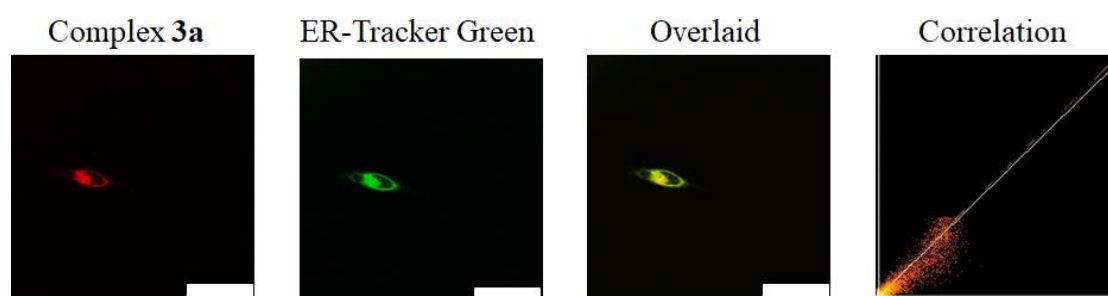


Figure S12. LSCM images of MDA-MB-231 cells incubated with complex **3a** (5 μ M; λ_{ex} = 405 nm, λ_{em} = 500 – 600 nm) at 37°C (left) or 4°C (right) for 3 h. Scale bar = 50 μ m.

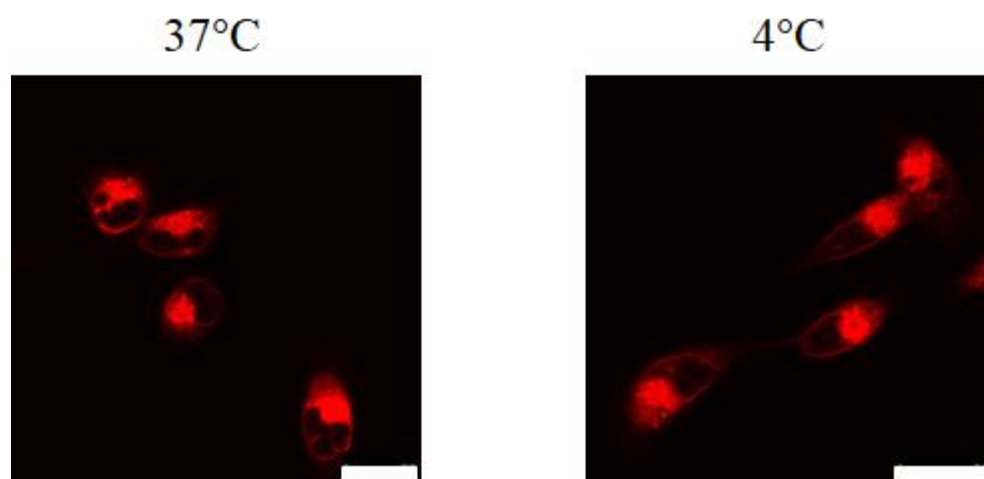


Figure S13. LSCM images of acidic autophagic vacuoles in MDA-MB-231 cells under different conditions. The cells were first pretreated without or with TCO-OH (100 μM) for 2 h, then incubated with complex **4** (10 μM) for 6 h, further left in fresh medium for 12 h, then remained in the dark or irradiated at 450 nm for 20 min (20 mW cm^{-2}), and subsequently incubated in the dark for 2 h. The samples were then stained with MDC (50 μM , 30 min; $\lambda_{\text{ex}} = 488 \text{ nm}$, $\lambda_{\text{em}} = 500 - 520 \text{ nm}$). Scale bar = 50 μm .

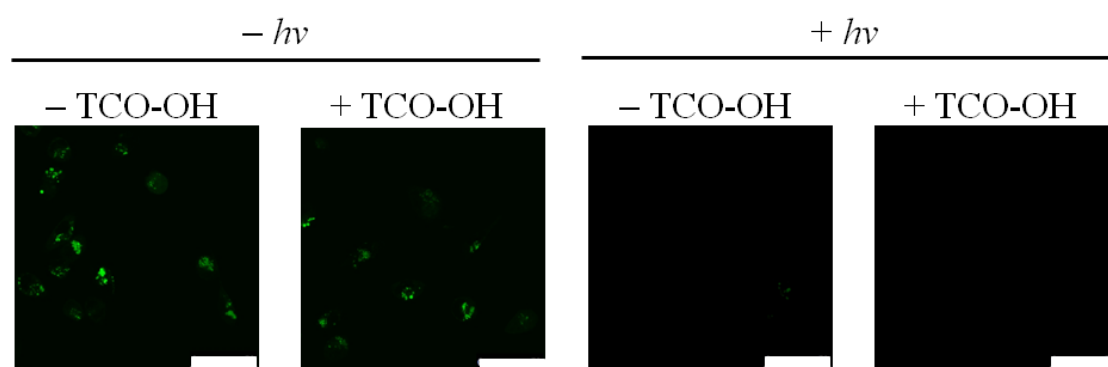


Figure S14. LSCM images of (a) CRT (CRT-Alexa 488 (10 μM , 1:200 solution, 2 h; λ_{ex} = 488 nm, λ_{em} = 500 – 520 nm); Hoechst 33258 (10 μM , 1 $\mu\text{g mL}^{-1}$, 10 min; λ_{ex} = 405 nm, λ_{em} = 420 – 450 nm)) and (b) HMGB1 (HMGB1-Alexa 488 (10 μM , 1:200 solution, 2 h; λ_{ex} = 488 nm, λ_{em} = 500 – 520 nm); Hoechst 33258 (10 μM , 1 $\mu\text{g mL}^{-1}$, 10 min; λ_{ex} = 405 nm, λ_{em} = 420 – 450 nm)). The cells were treated with complex **3a** (5 μM) for 6 h, left in fresh medium for 12 h, remained in the dark or were irradiated at 450 nm (20 mW cm^{-2}) for 20 min, and subsequently incubated in the dark for 2 h. Scale Bar = 25 μm .

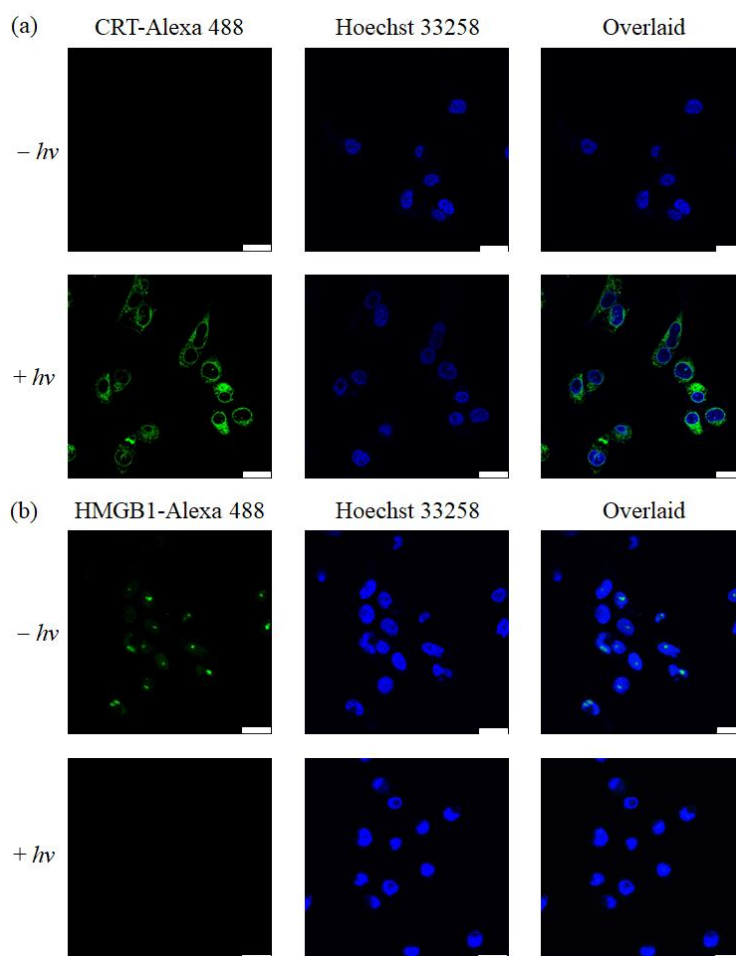


Figure S15. Extracellular ATP concentrations of MDA-MB-231 cells under different treatments. The cells were treated with complex **3a** (5 μ M) for 6 h, left in fresh medium for 12 h, remained in the dark or were irradiated at 450 nm (20 mW cm⁻²) for 20 min, and subsequently incubated in the dark for 2 h.

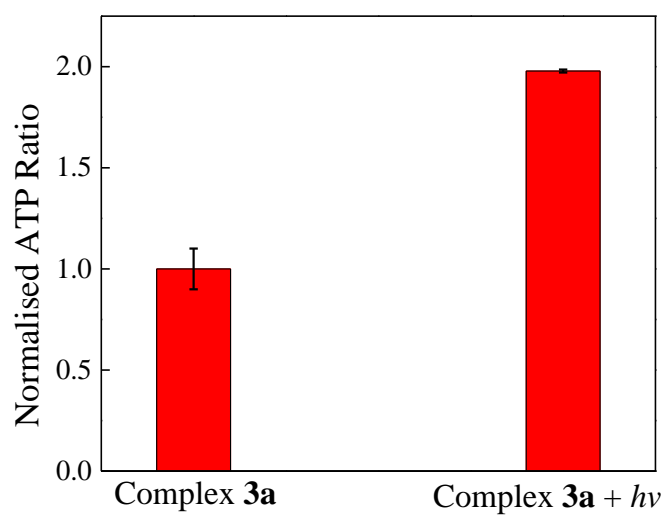


Figure S16. ^1H NMR spectrum of py-Tz-NHBoc in CDCl_3 at 298 K.

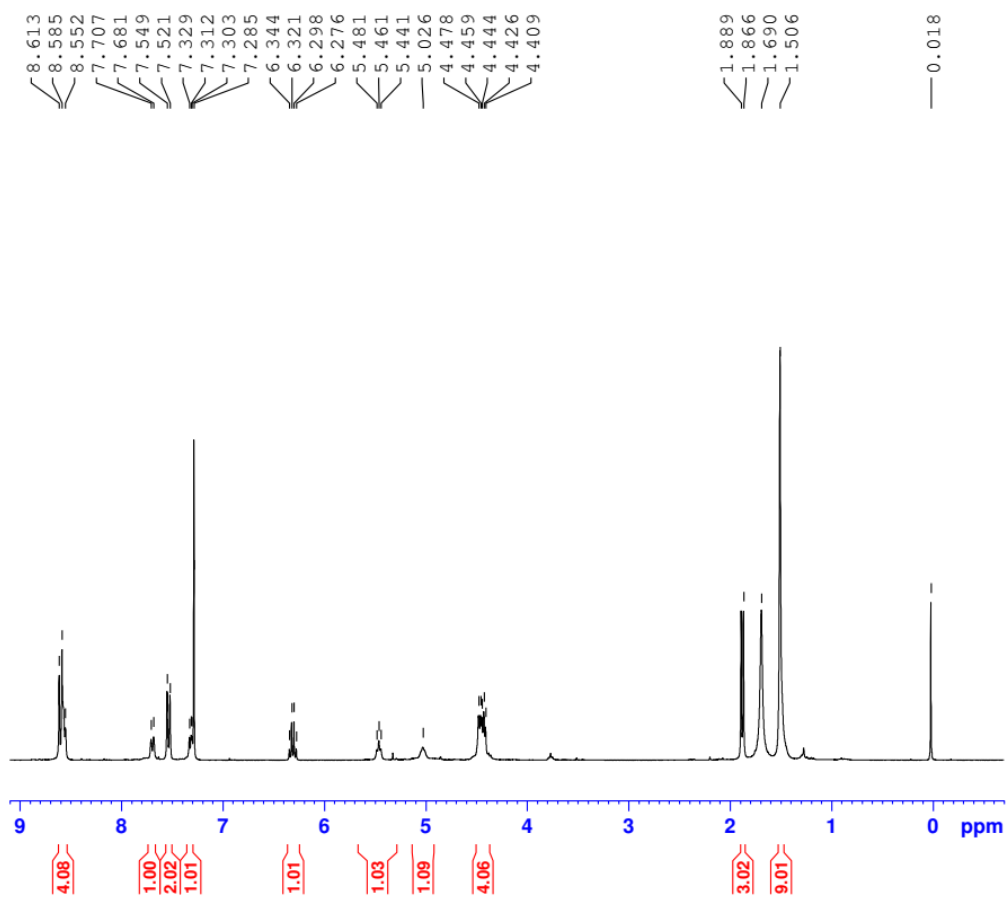


Figure S17. ^1H NMR spectrum of py-Tz-PEG₅₀₀₀ in CDCl_3 at 298 K.

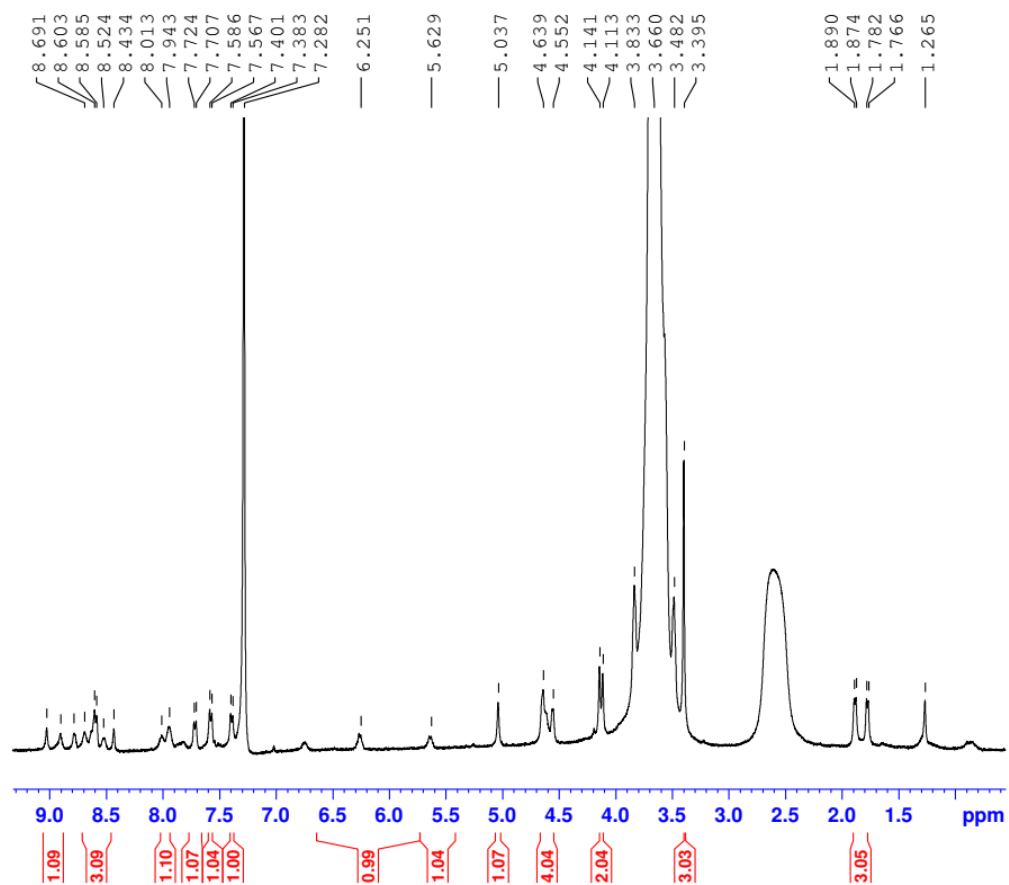


Figure S18. MALDI-TOF mass spectrum of py-Tz-PEG₅₀₀₀.

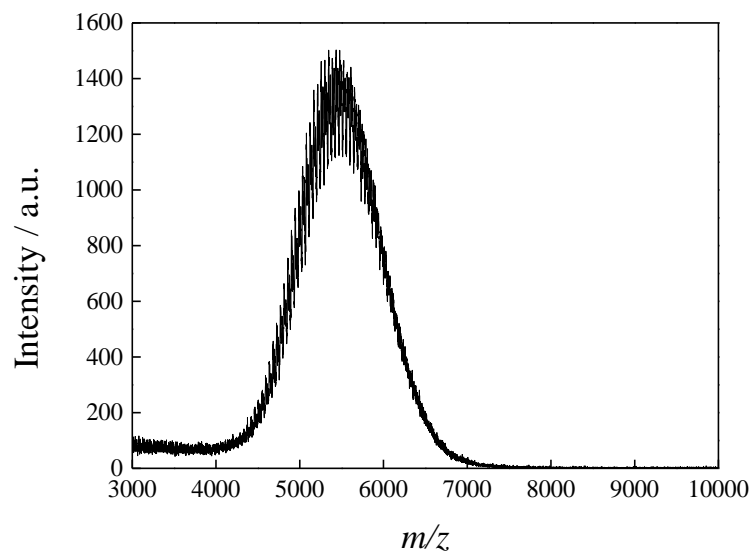


Figure S19. ^1H NMR spectrum of complex **1** in CDCl_3 at 298 K.

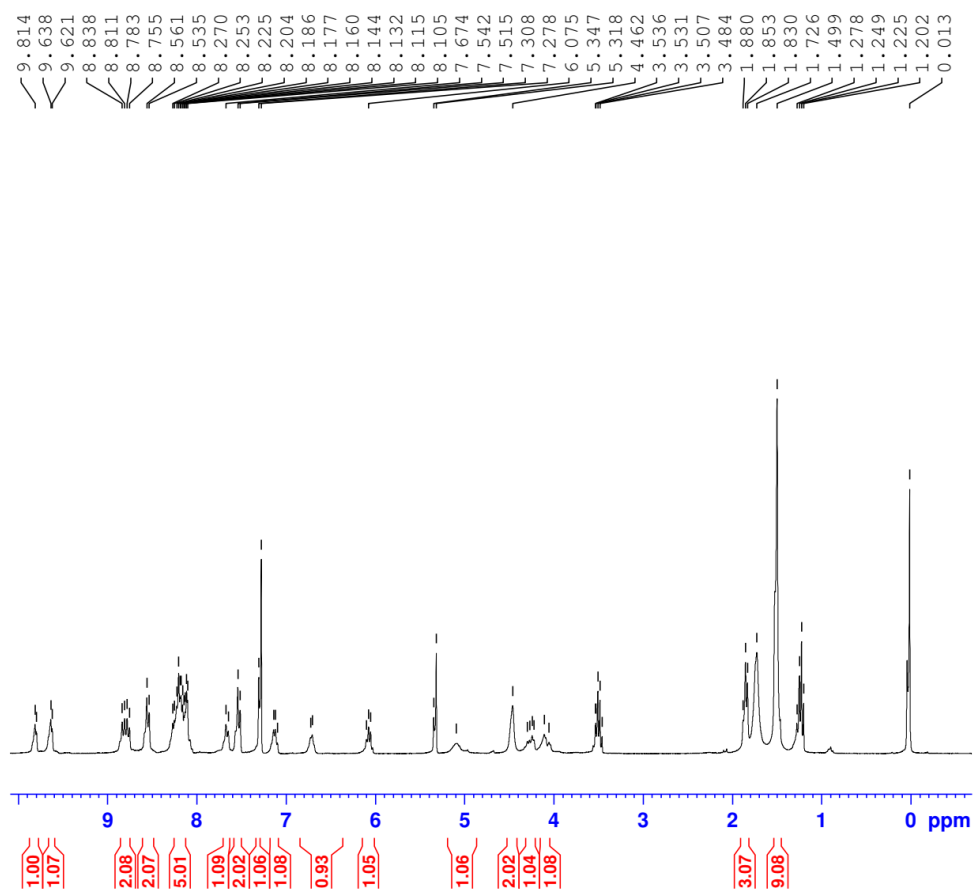


Figure S20. ^{13}C NMR spectrum of complex **1** in CDCl_3 at 298 K.

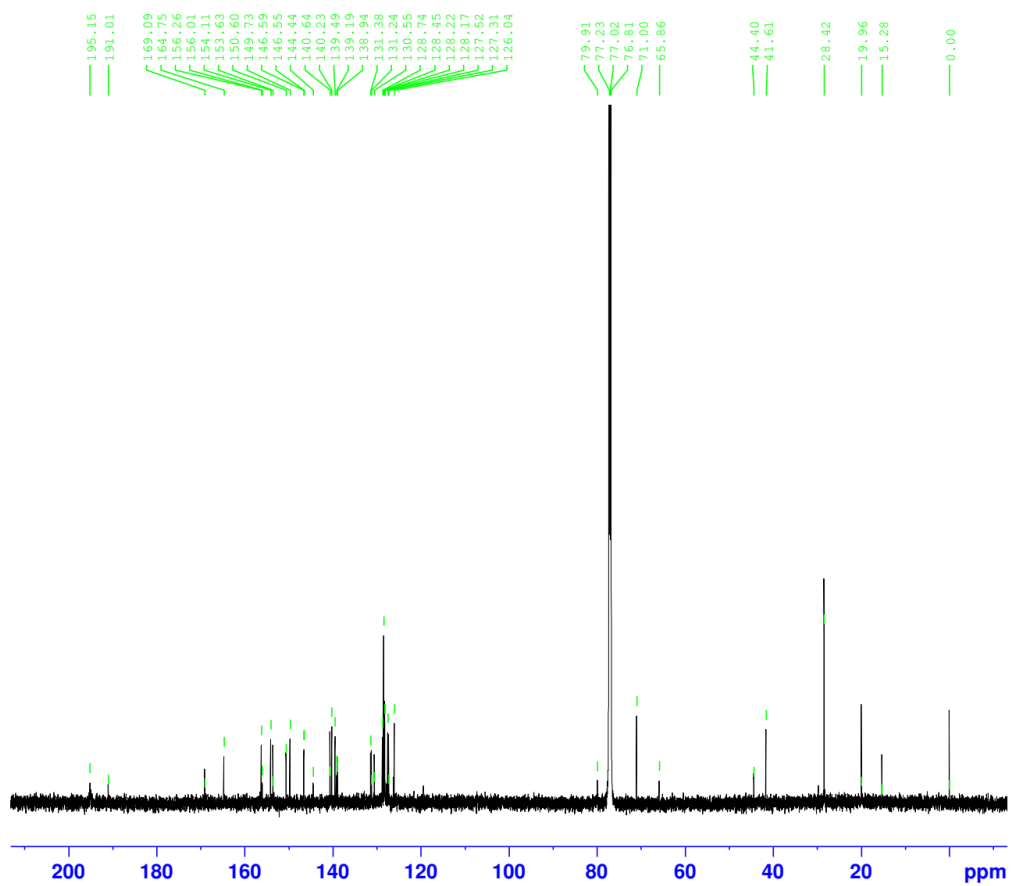


Figure S21. HR-ESI-mass spectrum of complex **1** in MeOH.

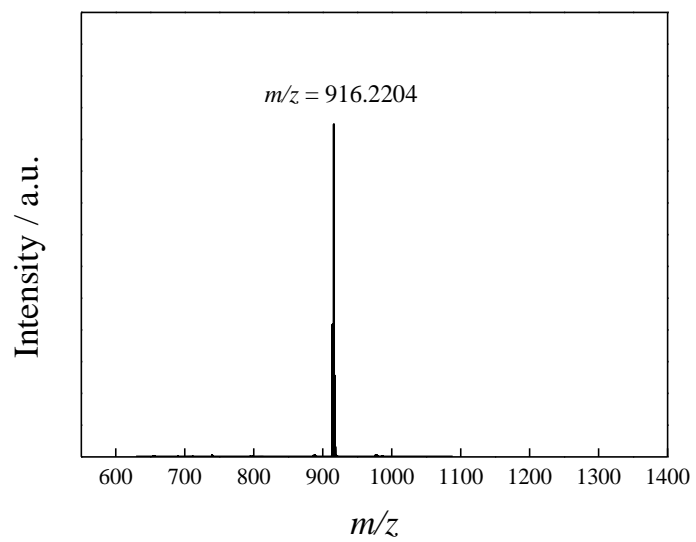


Figure S22. ^1H NMR spectrum of complex **2** in CDCl_3 at 298 K.

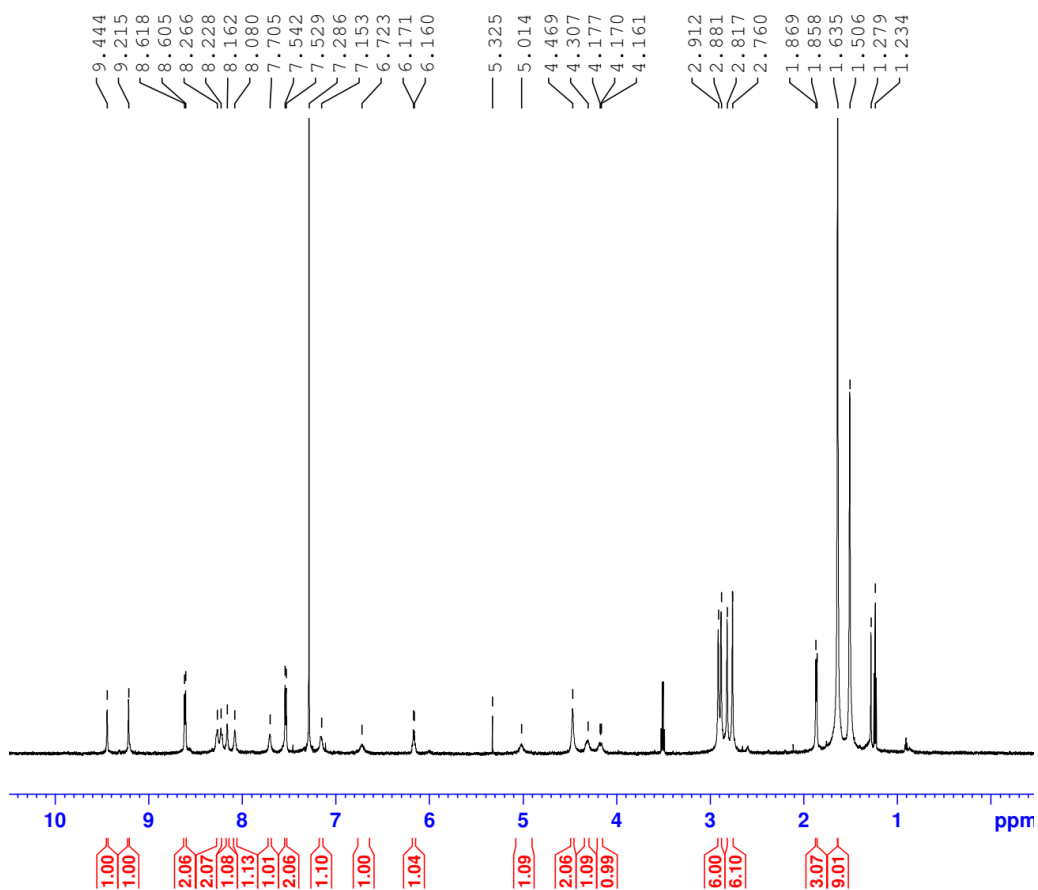


Figure S23. ^{13}C NMR spectrum of complex **2** in CDCl_3 at 298 K.

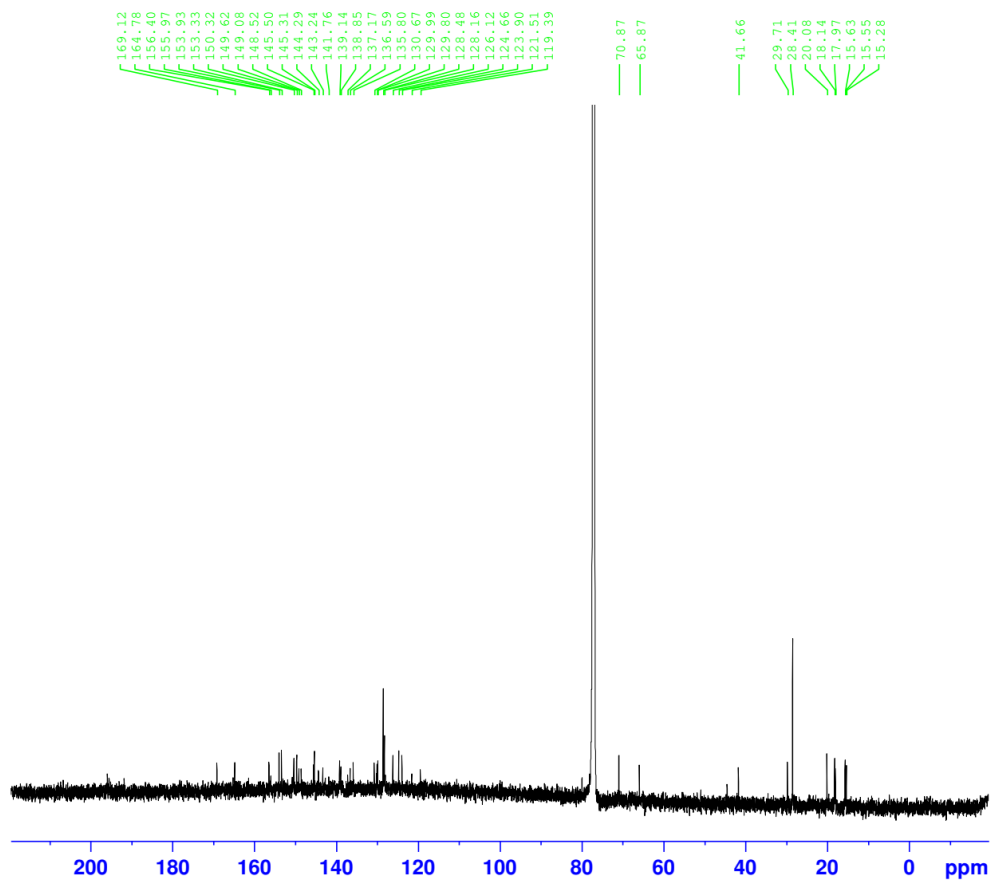


Figure S24. HR-ESI-mass spectrum of complex **2** in MeOH.

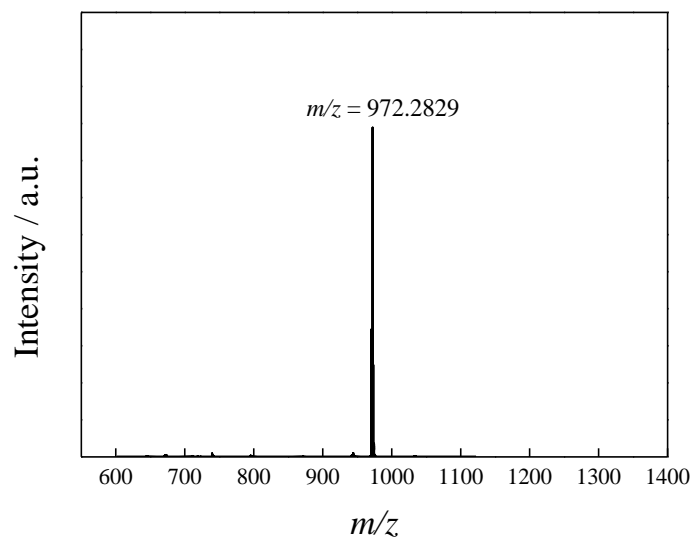


Figure S25. ^1H NMR spectrum of complex **3** in CDCl_3 at 298 K.

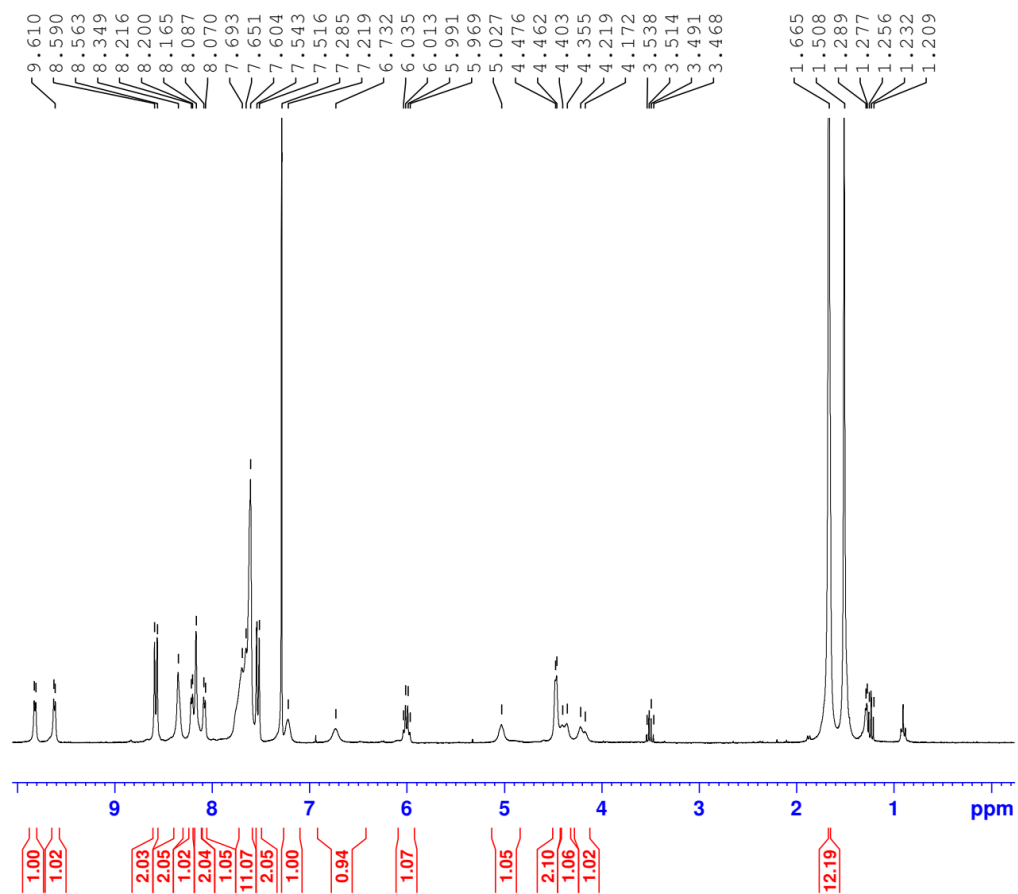


Figure S26. ^{13}C NMR spectrum of complex **3** in CDCl_3 at 298 K.

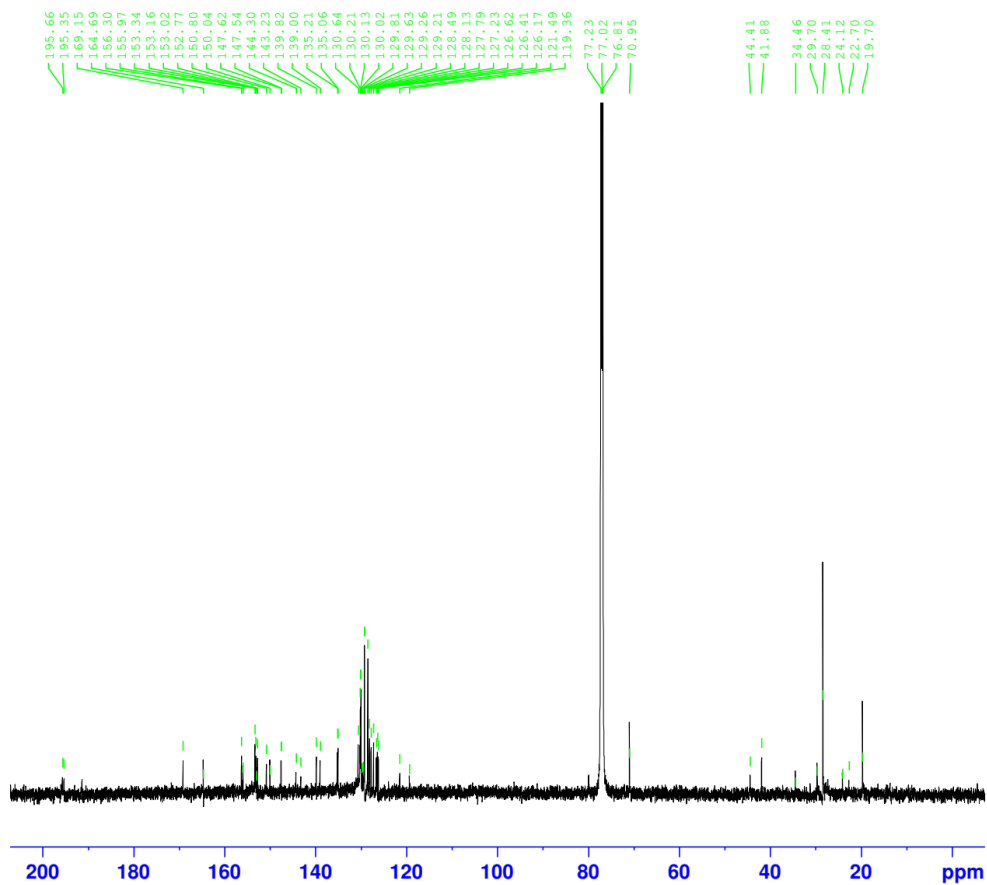


Figure S27. HR-ESI-mass spectrum of complex **3** in MeOH.

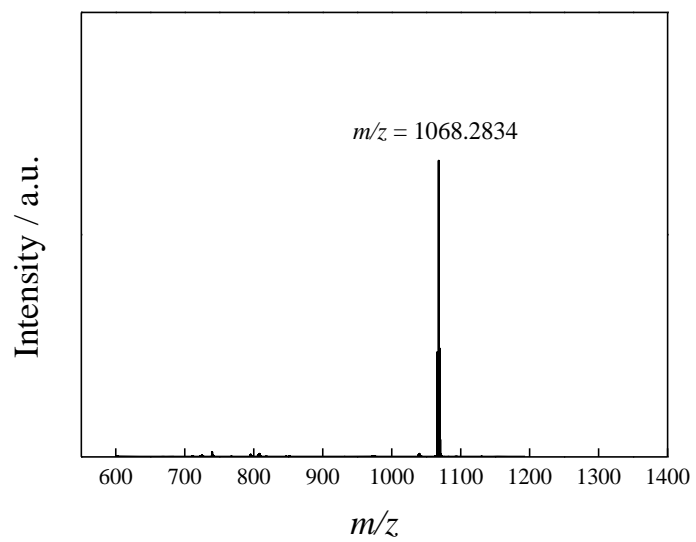


Figure S28. ^1H NMR spectrum of complex **4** in CDCl_3 at 298 K.

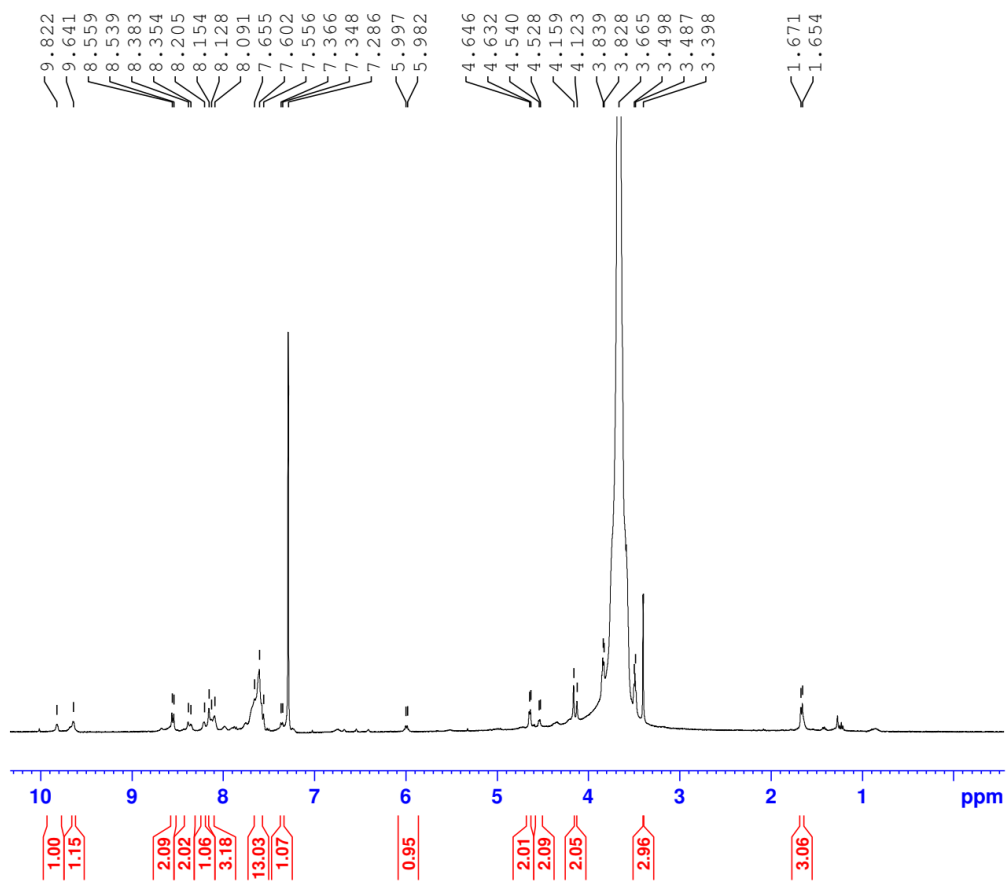
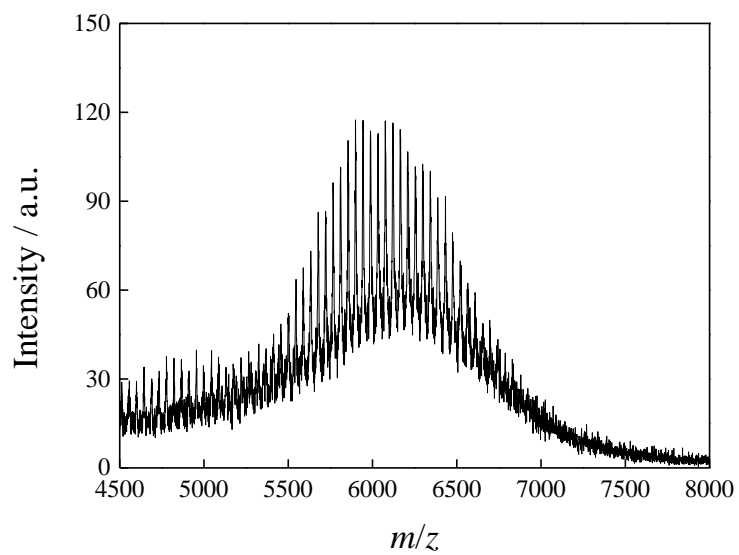


Figure S29. MALDI-TOF mass spectrum of complex **4**.



References

1. D. D. Perrin and W. L. F. Armarego, *Purification of Laboratory Chemicals*, Elsevier, Oxford, U. K., 2009.
2. A. H. A. M. van Onzen, R. M. Versteegen, F. J. M. Hoeben, I. A. W. Pilot, R. Rossin, T. Zhu, J. Wu, P. J. Hudson, H. M. Janssen, W. ten Hoeve and M. S. Robillard, *J. Am. Chem. Soc.*, 2020, **142**, 10955.
3. A. M.-H. Yip, J. Shum, H.-W. Liu, H. Zhou, M. Jia, N. Niu, Y. Li, C. Yu and K. K.-W. Lo, *Chem. Eur. J.*, 2019, **25**, 8970.
4. G. A. Crosby and J. N. Demas, *J. Phys. Chem.*, 1971, **75**, 991.
5. L. Wallance and D. P. Rillema, *Inorg. Chem.*, 1993, **32**, 3836.
6. V. A. Hackley and J. D. Clogston, *Characterization of Nanoparticles Intended for Drug Delivery*, Ed. S. E. McNeil, Springer, New York, 2011, **35**.
7. A. A. Abdel-Shafi, P. D. Beer, R. J. Mortimer and F. Wilkinson, *J. Phys. Chem. A*, 2000, **104**, 192.